- Caulobacter requires anionic sphingolipids and deactivation of fur to lose lipid A
- 3 Justin J. Zik^{1,12}, Sung Hwan Yoon^{2,13}, Ziqiang Guan³, Gabriele Stankeviciute Skidmore^{4,11},
- 4 Ridhi R. Gudoor^{5,6}, Karen M. Davies^{5,6,14}, Adam M. Deutschbauer⁷, David R. Goodlett^{2,8,9},
- 5 Eric A. Klein^{4,10,11} and Kathleen R. Ryan^{1,7,*}
- ¹Department of Plant & Microbial Biology, University of California, Berkeley, Berkeley, CA 94720
- 8 USA

2

- ²Department of Microbial Pathogenesis, University of Maryland School of Dentistry, Baltimore,
- 10 MD 21201 USA
- ³Department of Biochemistry, Duke University Medical Center, Durham, NC 27710
- 12 ⁴Center for Computational and Integrative Biology, Rutgers University-Camden, Camden, NJ
- 13 08102 USA
- ⁵Molecular Biosciences and Integrated Bioimaging Division, Lawrence Berkeley National
- 15 Laboratory, Berkeley, CA 94720 USA
- 16 Department of Molecular and Cell Biology, University of California, Berkeley, Berkeley, CA
- 17 94720 USA
- ⁷Environmental Genomics & Systems Biology Division, Lawrence Berkeley National Laboratory,
- 19 Berkelev, CA 94720 USA
- 20 *Department of Biochemistry & Microbiology, University of Victoria, Victoria, BC V8W 2Y2
- 21 Canada
- ⁹University of Victoria-Genome BC Proteomics Centre, Victoria, BC V8Z 7X8 Canada
- 23 ¹⁰Biology Department, Rutgers University-Camden, Camden, NJ 08102 USA
- 24 ¹¹Rutgers Center for Lipid Research, Rutgers University, New Brunswick, NJ 08901 USA
- 25 ¹²present address: Infectious Diseases Translational Research Programme, Department of
- 26 Microbiology and Immunology, Yong Loo Lin School of Medicine, National University of
- 27 Singapore, Singapore 117545, Singapore
- 28 ¹³present address: National Institute of Allergy and Infectious Diseases, Bethesda, MD 20892-
- 29 0421 USA
- 30 ¹⁴present address: Diamond Light Source Ltd. Harwell Science & Innovation Campus, Didcot,
- 31 Oxfordshire, OX11 0DE, UK
- *Correspondence: krr@berkeley.edu

Summary

Lipid A, the membrane-anchored portion of lipopolysaccharide, is an essential component of the outer membrane (OM) of nearly all Gram-negative bacteria. Here, we identify regulatory and structural factors that together permit *Caulobacter crescentus* to eliminate lipid A from its OM. Mutations in the ferric uptake regulator *fur* allow *Caulobacter* to survive in the absence of either LpxC, which catalyzes an early step of lipid A synthesis, or CtpA, a tyrosine phosphatase homolog which we find is needed for wild-type lipid A structure and abundance. Alterations in Fur-regulated processes, rather than iron status *per se*, underlie the ability to eliminate lipid A. Fitness of lipid A-deficient *Caulobacter* requires a previously uncharacterized anionic sphingolipid, ceramide phosphoglycerate (CPG), which also mediates sensitivity to the antibiotic colistin. Our results demonstrate that, in an altered regulatory landscape, anionic sphingolipids can support the integrity of a lipid A-deficient OM.

Introduction

Gram-negative bacteria are enclosed in a three-layer envelope, composed of the inner or cytoplasmic membrane (IM), a thin layer of peptidoglycan (PG), and an outer membrane (OM). The OM is an asymmetric bilayer, with phospholipids populating the inner leaflet and lipopolysaccharide (LPS) predominating in the outer leaflet. The canonical LPS structure, first described in *Escherichia coli*, consists of three segments: 1) lipid A, a hexa-acylated, phosphorylated glucosamine disaccharide anchored in the membrane; 2) a core oligosaccharide usually shared by members of the same species; and 3) a repeating polysaccharide (O-antigen) which can vary highly among strains of the same species (Whitfield and Trent, 2014). LPS confers robust barrier function upon the OM, making it inherently less permeable than the IM to small hydrophobic compounds. Barrier function has been ascribed to strong lateral interactions between LPS molecules mediated by packing of the saturated acyl chains of lipid A and a network of divalent cations coordinated by negatively charged groups, particularly those on lipid A or the core polysaccharide (Nikaido, 2003).

Although the O-antigen and core polysaccharide are nearly always dispensable, it is widely accepted that the lipid A portion of LPS is essential for Gram-negative bacterial viability. Some exceptions to this rule are species that possess a dual membrane system but naturally lack lipid A, such as *Borrelia burgdorferi, Treponema pallidum*, and *Sphingomonas spp*. (Kawahara et al., 1991; Kawasaki et al., 1994; Radolf and Kumar, 2018). Efforts to eliminate lipid A from *E. coli* strains have demonstrated that the intermediate molecule lipid IV_A is sufficient for viability, but only if the strain also has compensatory mutations that promote the

export of this species across the IM (Mamat et al., 2008; Meredith et al., 2006). To date lipid Adeficient mutants have been recovered in *Neisseria meningitidis*, *Moraxella catarrhalis*, and *Acinetobacter baumannii* (Moffatt et al., 2010; Peng et al., 2005; Steeghs et al., 1998). It remains unclear why at least a minimal lipid A structure is essential in some Gram-negative bacteria but not others.

Lipid A is synthesized by the highly conserved Raetz pathway (Whitfield and Trent, 2014), yet significant variation exists in lipid A structures. In many species, mechanisms exist to modify the 1- and 4□-phosphoryl groups of lipid A to decrease its negative charge and reduce susceptibility to cationic antimicrobial peptides (Moffatt et al., 2019). In a few species, replacement of the 1- and/or 4□-phosphoryl groups of lipid A with sugars is constitutive (De Castro et al., 2008; Plötz et al., 2000). The predominant lipid A species in the alphaproteobacterium *Caulobacter crescentus* (Smit et al., 2008) varies from that of *E. coli* (Qureshi et al., 1988) in that the central glucosamine disaccharide is replaced by two 2,3-diamino-2,3-dideoxy-D-glucopyranose (GlcN3N) residues, and the 1- and 4□-phosphates are replaced by galactopyranuronic acid (GalpA) residues.

The tyrosine phosphatase homolog ctpA (for \underline{C} aulobacter \underline{t} yrosine \underline{p} hosphatase \underline{A}) is essential for viability and is implicated in cell envelope maintenance, but its molecular function remains unknown (Shapland et al., 2011). Depletion of ctpA causes extensive OM blebbing, failure to resolve PG at the division site, and cell death. Here, we show that ctpA is required for the wild-type structure and abundance of lipid A. A screen for suppressors of ctpA essentiality recovered strains with null mutations in the O-antigen biosynthetic pathway or in the ferric uptake regulator fur. Surprisingly, mutations in fur also permitted the deletion of lpxC, which encodes an otherwise essential enzyme catalyzing the first committed step in lipid A synthesis. $\Delta ctpA$ and $\Delta lpxC$ strains containing suppressor mutations have significantly reduced or undetectable levels of lipid A, respectively.

To identify mechanisms that promote survival in the absence of lipid A, we used random barcode transposon-site sequencing (RB-Tnseq) to identify genes important for fitness when lipid A synthesis is chemically inhibited. Interestingly, we obtained several hits in genes required for sphingolipid synthesis in *Caulobacter* (Stankeviciute et al., 2019, 2021). Since *Sphingomonads* naturally lack LPS and bear anionic sphingolipids on the cell surface (Kawasaki et al., 1994), we hypothesized that anionic sphingolipids could support viability in the *Caulobacter* $\Delta lpxC$ strain. Indeed, we identified a previously unknown sphingolipid species, ceramide phosphoglycerate, which is a critical fitness factor in the absence of lipid A. Further,

we found that ceramide phosphoglycerate, rather than LPS, underlies *Caulobacter's* sensitivity to the cationic antimicrobial peptide colistin.

Results

Suppressor mutations affecting fur or O-antigen synthesis permit the loss of ctpA

We used a CtpA depletion strain (see Methods, CtpA depletion strain) to identify mutations that would support *Caulobacter* viability in the absence of CtpA (Shapland et al., 2011). When depleting CtpA by transferring cells from xylose-supplemented rich medium (PYEX) to dextrose-supplemented rich medium (PYED), KR3906 exhibits division defects, significant OM blebbing, and death (**Fig. 1**). We UV-mutagenized KR3906, plated survivors on solid PYED medium to deplete CtpA, and grew the recovered colonies in PYED liquid medium to allow loss of the plasmid bearing *ctpA*. Isolates that had successfully lost the plasmid were identified via chloramphenicol sensitivity and the inability to PCR-amplify *ctpA* (**Fig. 1A**). Genome resequencing of 17 confirmed suppressors yielded 15 strains with mutations in nine genes predicted to participate in O-antigen biosynthesis, one strain with a single mutation in *fur*, encoding the ferric uptake regulator, and one strain harboring a mutation in *fur* along with a mutation in an O-antigen biosynthetic gene (**Table S1**). Due to the frequent occurrence of frameshift or nonsense mutations, we assumed that each mutation disrupted the function of the affected gene.

We chose the following candidate suppressors for further analysis: (i) *CCNA_00497*, encoding a predicted rhamnosyl transferase necessary for wild-type levels of O-antigen containing smooth LPS (S-LPS) (Hershey et al., 2019); (ii) *CCNA_01553*, encoding a glycosyltransferase which initiates O-antigen synthesis on undecaprenyl-phosphate (Toh et al., 2008); (iii) *CCNA_03733*, encoding a homolog of *manC* involved in synthesizing the activated sugar GDP-D-mannose (Samuel and Reeves, 2003), which is present in the core oligosaccharide and O-antigen of *Caulobacter* S-LPS (Jones et al., 2015); and iv) *CCNA_00055*, encoding the iron-responsive transcriptional regulator Fur (da Silva Neto et al., 2013). We individually deleted these genes in the CtpA depletion strain KR3906 while propagating the strains on PYEX.

To determine how each deletion affects cells during acute CtpA depletion, we shifted each mutant onto liquid or solid PYED medium and observed cell morphology and viability (**Fig.** 1). Compared to CtpA depletion in KR3906, acute depletion of CtpA in the Δfur mutant caused much less OM blebbing, but still yielded elongated cells indicative of a division defect (**Fig. 1C**). Surprisingly, neither OM blebbing nor cell chaining/elongation was markedly improved when

CtpA was depleted from the strains lacking *CCNA_00497*, *CCNA_01553*, or *CCNA_03733*. Despite the persistence of one or more morphological defects, deletion of *fur*, *CCNA_01553*, or *CCNA_03733* significantly improved cell viability during depletion of CtpA on solid PYED medium (**Fig. 1B**). In contrast, the deletion of *CCNA_00497* only weakly improved survival on PYED medium. Two independent point mutations in *CCNA_00497* were isolated in the suppressor screen, but each mutant also harbored 1-2 other mutations (**Table S1**) that may have contributed to the fitness of the original isolates.

To acquire stable $\triangle ctpA$ derivatives of each suppressor strain constructed above, we plated each new mutant on PYED medium and screened viable colonies for loss of the ctpA-bearing plasmid. The OM of each stable $\triangle ctpA$ strain was smooth with minimal blebbing, but chains of cells were still prevalent in the $\triangle CCNA_01553$ and $\triangle fur$ mutants (**Fig. 1D**). These reconstituted suppressor strains are morphologically similar to the original isolates containing point mutations in the same genes (**Fig. S1A**). Suppressed $\triangle ctpA$ mutants grow more slowly than the wild-type strain NA1000 and the corresponding $ctpA^+$ strains, but all achieve similar stationary phase densities in PYE medium (**Fig. S1B**). As expected, restoring the expression of fur, $CCNA_00497$, or $CCNA_03733$ using a xylose-inducible promoter reduced the viability of each corresponding stable $\triangle ctpA$ strain (**Fig. S1C**). Thus, null mutations affecting fur or O-antigen biosynthesis allow Caulobacter to survive in the absence of ctpA.

To confirm the functions of suppressor genes predicted to be involved in O-antigen synthesis, we deleted the individual genes in a control strain lacking sspB (see Methods, CtpA depletion strain). Whole-cell lysates treated with proteinase K were probed with antibodies recognizing S-LPS (**Fig. S2A**) or stained with Pro-Q Emerald 300 to detect carbohydrates (**Fig. S2B**). As previously observed, a control strain $\Delta CCNA_01068$ (wbqA) and the $\Delta CCNA_01553$ mutant lacked S-LPS (Awram and Smit, 2001), which migrates as a single high-molecular weight species in *Caulobacter* (Walker et al., 1994). Mutations in $CCNA_00497$ or $CCNA_03733$ caused partial or complete elimination of S-LPS, respectively. S-LPS was restored to each mutant by xylose-driven complementation of the respective genes (**Fig. S2C**). In contrast to strains with mutations in $CCNA_00497$, $CCNA_01553$, or $CCNA_03733$, the Δfur $\Delta sspB$ mutant contained wild-type levels of S-LPS (**Fig. S2A-C**), indicating that fur mutations do not suppress the lethality of $\Delta ctpA$ by eliminating the O-antigen.

We propose that a low-molecular weight band in most lysates represents lipid A + core polysaccharide (**Fig. S2B and S2C**, **). This inference is supported by the band pattern in the $\Delta CCNA~03733~(manC)$ mutant. The core oligosaccharide of *Caulobacter* LPS contains a single

penultimate mannose residue (Jones et al., 2015); thus, the reduced size of the indicated band for $\triangle CCNA_03733$ (**Fig. S2B and S2C**, *) may arise from an incomplete core oligosaccharide.

Suppressor mutations permit ΔctpA and ΔlpxC strains to survive with little or no lipid A ctpA is transcribed divergently from an operon containing msbA, lpxJ, kdtA, and lpxK (Zhou et al., 2015), which in other bacteria participate in the synthesis and export of lipid A + core polysaccharide (Whitfield and Trent, 2014). Like ctpA, these genes are essential for Caulobacter viability (Christen et al., 2011). Since CtpA depletion results in OM defects, and suppressor mutations were identified in O-antigen biosynthetic genes, we hypothesized that ctpA is required for some aspect of LPS synthesis or export.

We performed hot aqueous-phenol extraction of LPS from suppressor mutants lacking ctpA, along with their $ctpA^+$ counterparts, and analyzed them by PAGE and Pro-Q Emerald 300 staining. Full-length S-LPS was recovered from NA1000, $\Delta sspB$, and $\Delta fur \Delta sspB$ (**Fig. 2B**, ***), whereas only smaller LPS species were present in the $\Delta sspB$ strains lacking $CCNA_00497$, $CCNA_01553$, or $CCNA_03733$. Interestingly, all $\Delta ctpA$ strains harboring suppressor mutations were deficient in low-molecular weight species that could represent lipid A +/- core oligosaccharide (**Fig. 2B**). We therefore used the Limulus Amebocyte Lysate (LAL) assay to measure lipid A abundance in live *Caulobacter* strains. The stable $\Delta ctpA$ mutants contained approximately 1,000-fold less lipid A than NA1000 or the corresponding $ctpA^+$ strains (**Fig. 2A**).

Since Δ*ctpA* suppressor mutants could survive with drastically reduced amounts of lipid A, we asked if mutations in *fur* or O-antigen synthesis could allow *Caulobacter* to lose lipid A entirely. LpxC catalyzes the first committed step in lipid A synthesis, removal of the 2-acetyl group from acylated UDP-GlcNAc (Whitfield and Trent, 2014). The *lpxC* homolog *CCNA_02064* is essential for viability in wild-type *Caulobacter* (Christen et al., 2011). We constructed an LpxC depletion strain (KR4007) analogous to the CtpA depletion strain. We subsequently deleted *fur*, *CCNA_00497*, *CCNA_01553*, or *CCNA_03733* in this strain and examined the effects of acute LpxC depletion during growth in PYED. In the absence of candidate suppressor mutations, LpxC depletion yielded chains of cells with extensive membrane blebs. Cells lacking a gene for O-antigen synthesis still showed membrane blebs and chaining when LpxC was depleted (**Fig. 3A**). Cells lacking *fur* had far fewer OM blebs upon LpxC depletion but were still frequently elongated or chained (**Fig. 3A**). These morphologies are generally similar to those seen during CtpA depletion, but unlike CtpA, only Δ*fur* allowed significant growth of the LpxC depletion strain on solid PYED medium (**Fig. 3B**).

When we attempted to isolate stable $\Delta lpxC$ mutants using the same outgrowth and screening process as for $\Delta ctpA$, only the strain harboring a Δfur mutation permitted complete loss of lpxC. We initially recovered two stable $\Delta lpxC$ isolates from a depletion strain harboring $\Delta CCNA_00497$, but genome resequencing revealed that these strains had acquired additional mutations in fur (**Table S2**). As in $\Delta ctpA$ Δfur $\Delta sspB$, the stable $\Delta lpxC$ Δfur $\Delta sspB$ mutant still formed chains (**Fig. 1D**), and xylose-driven fur expression induced lethality in this background (**Fig. 3C**).

Background levels of lipid A were detected in Δ*lpxC* Δ*fur* Δ*sspB* cells in the LAL assay (**Fig. 2A**), strongly suggesting that lipid A is absent. To corroborate this result, we extracted LPS species by three distinct methods, separated them by PAGE, and stained with Pro-Q Emerald 300. Hot aqueous-phenol extracts of Δ*lpxC* Δ*fur* Δ*sspB* cells were deficient in S-LPS and putative lipid A +/- core species (**Fig. 2B**). However, unknown carbohydrate-containing species were extracted by this method. Extraction of free lipid A (El Hamidi et al., 2005) revealed that a species of ~1800 Da, consistent with the mass of *Caulobacter* lipid A (Smit et al., 2008), is present in NA1000 but absent from Δ*lpxC* Δ*fur* Δ*sspB* (**Fig. 2C**, **left**). Again, however, unidentified carbohydrate species were present in these extracts. Lastly, the method of Darveau and Hancock (Darveau and Hancock, 1983) yielded a single rough LPS species which was present in NA1000 and absent from Δ*lpxC* Δ*fur* Δ*sspB* (**Fig. 2C**, **right**); this method resulted in no unidentified contaminants. Although some *Caulobacter* extracts contain unidentified lipids, these assays together strongly imply that lipid A is absent from the Δ*lpxC* Δ*fur* Δ*sspB* mutant. Xylose-driven expression of *lpxC* or *ctpA* restored the production of lipid A-containing species to Δ*lpxC* Δ*fur* Δ*sspB* or Δ*ctpA* Δ*CCNA_01553* Δ*sspB*, respectively (**Fig. 2D**).

Lipid A extracts from $\triangle ctpA$ $\triangle fur$ $\triangle sspB$, $\triangle lpxC$ $\triangle fur$ $\triangle sspB$, and control strains were further analyzed by matrix-assisted laser desorption/ionization tandem mass spectrometry (MALDI-MS/MS). Wild-type NA1000, $\triangle sspB$, and $\triangle fur$ $\triangle sspB$ extracts contained predominantly the full-length lipid A (m/z 1874, (Smit et al., 2008) and lesser amounts of an ion at m/z 1858 that differs from 1874 by 16 m/z, consistent with the absence of one hydroxyl group (**Fig. S3A-C**). MALDI-MS analyses of lipid A extracts from $\triangle ctpA$ $\triangle fur$ $\triangle sspB$ cells revealed no ions consistent with full-length Caulobacter lipid A, but identified ions at m/z 1682 and m/z 1486 (**Fig. S3D**) that appeared to be missing the GalpA residues at the 1 and 4 \square positions. Tandem MS analysis of these ions revealed mass losses consistent with phosphates, as would be expected for canonical lipid A structures. Although additional characterization is needed, our results suggest that Caulobacter mutants lacking CtpA produce an incomplete lipid A species which retains phosphate at the 1 and 4 \square positions, and which lacks one or more of the secondary

phospholipids. While these incomplete lipid A species were detectable by mass spectrometry, gel electrophoresis and LAL assays indicate that they are much less abundant than the lipid A in wild-type strains.

Lipid A extracts from the $\Delta lpxC$ Δfur $\Delta sspB$ mutant yielded no ions consistent with wild-type lipid A and instead contained an unknown lipid (**Fig. S3E**, m/z 1412). Numerous attempts to interpret the structure of this ion using the same type of tandem MS data as used in Fig. S3A-D failed to generate a structural hypothesis resembling obvious choices such lipid A derivatives or cardiolipin. Again, it is important to note that while this unknown ion was detected by mass spectrometry, gel electrophoresis and LAL assays together indicate that lipid A is absent from $\Delta lpxC$ Δfur $\Delta sspB$ cells.

Lipid A-deficient Caulobacter mutants produce a three-layer cell envelope

We analyzed NA1000, $\Delta ctpA$ Δfur $\Delta sspB$ and $\Delta lpxC$ Δfur $\Delta sspB$ strains via electron cryotomography to assess the effects of mutations on cell envelope structure (**Movies S1-S4**). As expected, the S-layer is absent from both mutants due to the loss of its O-antigen attachment site (Walker et al., 1994). Despite drastic reductions in lipid A levels, the $\Delta ctpA$ Δfur $\Delta sspB$ and $\Delta lpxC$ Δfur $\Delta sspB$ mutants still generate a three-layer cell envelope, including an OM (**Fig. 2E**). Although much less severe than during acute CtpA depletion (**Movie S4**), membrane blebs were often observed at the cell poles or division sites in $\Delta ctpA$ Δfur $\Delta sspB$ and $\Delta lpxC$ Δfur $\Delta sspB$ cells (**Fig. 2E**). A significant proportion of ctpA and lpxC mutant cells exhibited defects in stalk structure or IM distortions at the pole or midcell (N = 100; $\Delta ctpA$ Δfur $\Delta sspB$: 61%; $\Delta lpxC$ Δfur $\Delta sspB$: 51%; NA1000: 4%).

Fur-regulated processes, rather than available iron levels, control the conditional essentiality of lipid A

LPS defects are usually associated with increased chemical sensitivity (Nikaido, 2003). Mutations in *fur* or O-antigen synthesis genes did not appreciably increase chemical sensitivity compared to NA1000, while strains lacking *ctpA* or *lpxC* had greater sensitivity to a subset of antibiotics and to all tested detergents (**Fig. 4A**). In sharp contrast, the $\Delta lpxC$ Δfur $\Delta sspB$ strain and $\Delta ctpA$ $\Delta sspB$ strains with suppressor mutations were much less susceptible to CHIR-090, an inhibitor of LpxC (McClerren et al., 2005) (**Fig. 4B**). We infer that suppressed $\Delta lpxC$ and $\Delta ctpA$ mutants are relatively insensitive to CHIR-090 because they already produce little lipid A or lack the target enzyme.

In agreement with its ability to suppress the lethality of $\Delta lpxC$ and $\Delta ctpA$ mutations, the Δfur allele by itself greatly reduced the sensitivity of *Caulobacter* to CHIR-090 (**Fig. 4B**). Fur senses available Fe²⁺ by reversibly binding a [2Fe-2S] cluster (Fontenot et al., 2020). We therefore asked whether iron limitation could mimic the phenotypes of a Δfur mutant. Culturing NA1000 with the iron chelator 2,2'-dipyridyl reduced its susceptibility to CHIR-090 to match that of the Δfur mutant (**Fig. 4B**). Neither depleting LpxC in fur^+ cells nor inducing fur in $\Delta lpxC$ Δfur $\Delta sspB$ cells caused a reduction in viability in the presence of 2,2'-dipyridyl (**Fig. 4C, D**). The NA1000, $\Delta sspB$, and Δfur $\Delta sspB$ strains cultured in 2,2'-dipyridyl retained LPS and lipid A +/-core species (**Fig. 4E**). Therefore, low iron availability does not induce the loss of lipid A, but is sufficient to maintain *Caulobacter* viability when lipid A is eliminated by chemical or genetic means.

In diverse bacteria, Fur inhibits the expression of iron uptake systems and promotes the expression of proteins that utilize iron, contributing to iron homeostasis (Andrews et al., 2013). Because they are impaired in iron sensing, *fur* mutants of other bacteria accumulate more available iron than the corresponding wild-type strains (Liu et al., 2020; Wofford et al., 2019). We measured available iron levels using a streptonigrin (SNG) sensitivity assay (Justino et al., 2007; Nachin et al., 2001), because SNG killing is linked to the intracellular formation of oxygen radicals in the presence of iron (Hassett et al., 1987; Yeowell and White, 1982). Growth of the Δfur and $\Delta fur \Delta sspB$ strains was almost completely inhibited by 0.25 µg/ml SNG, while NA1000 was only mildly inhibited (**Fig. 4F**), consistent with higher levels of available iron in Δfur mutants. These findings indicate that both excess available iron (in *fur* mutants) and iron depletion (by 2,2-dipyridyl) are compatible with the elimination of lipid A. Since *fur* deletion and iron chelation have the same effect on Fur-regulated gene expression, but opposite effects on Furindependent iron signaling (**Fig. 4G**), this implies that iron-mediated processes regulated by Fur are specifically responsible for the survival of lipid A-deficient *Caulobacter* (Leaden et al., 2018; da Silva Neto et al., 2013).

RB-Tnseq identifies sphingolipid synthesis genes needed for fitness when lipid A synthesis is chemically inhibited

To identify additional factors that promote the survival of lipid A-deficient *Caulobacter*, we challenged an RB-Tnseq library constructed in NA1000 (Price et al., 2018) with CHIR-090. Individual barcode frequencies were measured by high-throughput sequencing before each trial and after growth in either PYE or PYE + 2 μ g/ml CHIR-090. To identify genes that are particularly important when LpxC is inhibited, we averaged and compared the gene fitness

scores (Wetmore et al., 2015) from three trials in each condition (**Fig. 5A**). We anticipated that mutations in *fur* would increase fitness in CHIR-090, but the NA1000 RB-Tnseq library contained no insertions in *fur*. Surprisingly, nearly all genes known to be regulated by Fur (Leaden et al., 2018; da Silva Neto et al., 2013) had similar fitness scores in unstressed and CHIR-090-exposed cultures (**Fig. 5A**).

Focusing on genes whose average fitness scores were \geq 1 point lower in CHIR-090-treated cultures than in control cultures, we identified five genes involved in sphingolipid synthesis: spt ($CCNA_01220$), acyl-carrier protein (acp, $CCNA_01221$), cerR ($CCNA_01222$), ACP-synthetase (acps, $CCNA_01223$), and bcerS ($CCNA_01212$) (Olea-Ozuna et al., 2021; Stankeviciute et al., 2021). Additionally, fitness scores were lower for transposon insertions in a neighboring operon of three uncharacterized genes predicted to modify lipids ($CCNA_01217_01219$, Marks et al., 2010) (**Fig. 5A**). To examine the roles of genes in the uncharacterized operon, we constructed unmarked deletions in the NA1000 and $\Delta fur \Delta sspB$ backgrounds and complemented them with the corresponding genes expressed from the inducible vanA promoter (Thanbichler et al., 2007). Loss of spt, $CCNA_01217$, $CCNA_01218$, or $CCNA_01219$ greatly increased the susceptibility to CHIR-090, either in NA1000 or in $\Delta fur \Delta sspB$ cells (**Fig. 5B**), and expression of the complementing gene from the vanA locus restored the wild-type level of susceptibility, validating the RB-Tnseq results.

Mutations in *CCNA_01217-01219* or *spt* could increase CHIR-090 sensitivity via distinct mechanisms: by damaging the cell's permeability barrier and giving easier access to CHIR-090, by making it more difficult for cells to grow after lipid A synthesis is inhibited, or both. To eliminate changes in drug access as a factor in the experiment, we measured the effects of *CCNA_01217*, *CCNA_01218*, and *spt* upon cell viability when LpxC was depleted. We deleted individual genes in the strain Δ*lpxC* Δ*fur* Δ*sspB* + P*xyl-lpxC::3xFLAG-ssrA* (KR4091) and complemented them with *vanA*-driven copies as described above. The parent strain lacks *fur* and grows in PYED medium when LpxC is depleted. In contrast, KR4091 lacking *CCNA_01217* or *spt* grew poorly in PYED medium, and growth in PYED was fully or partially restored by expressing the complementing gene from the vanillate promoter (**Fig. 5C**). KR4091 lacking *CCNA_01218* grew poorly in PYEX and PYED media without vanillate, indicating that KR4091 requires *CCNA_01218* for fitness even when LpxC is produced. Growth was improved by vanillate-driven expression of *CCNA_01218* (**Fig. 5C**). Since this assay does not rely on an exogenous chemical, we conclude that *CCNA_01217-8* and *spt* are critical for the fitness of lipid A-deficient *Caulobacter*, not simply for the exclusion of CHIR-090.

CCNA_01217-01219 convert neutral ceramide to an anionic sphingolipid, ceramide phosphoglycerate

The importance of Spt for viability in the absence of lipid A indicated a role for sphingolipids in this phenotype. Since *Sphingomonads* produce anionic glycosphingolipids (GSLs) on the outer membrane (Kawasaki et al., 1994), we initially hypothesized that *Caulobacter* responds to *IpxC* deletion by upregulating GSL production. However, neither *Caulobacter* sphingolipid glycosyltransferase (*sgt1* or *sgt2*, Stankeviciute et al., 2019) was important for the fitness of CHIR-090-treated cells. A careful analysis of the *Caulobacter* lipidome revealed a previously unidentified sphingolipid species, ceramide phosphoglycerate (**Fig. 6A**). In fact, we identified two forms of this lipid containing either one or two phosphoglycerate moieties (**Fig. 6A**) that we have designated CPG and CPG2. LC/MS/MS analysis confirmed the proposed structures of these lipids (**Fig. 6B**).

To determine whether CCNA 01217-01219 are involved in CPG/CPG2 synthesis, we analyzed lipid extracts from mutant and complemented mutant strains. Deletion of CCNA_01217 resulted in the loss of CPG2 but had no effect on CPG (Fig. 6C). CCNA_01217 has a conserved phosphatidylglycerophosphate synthase (PgsA) domain which is normally involved in phosphatidylglycerol (PG) synthesis. PG is the dominant phospholipid in Caulobacter (Stankeviciute et al., 2019), but the essential PgsA ortholog CCNA 03002 is likely responsible for PG synthesis (Christen et al., 2011; Marks et al., 2010). Thus, we conclude that CCNA 01217 adds the second phosphoglycerate to form CPG2. Deletion of CCNA 01218 led to the loss of CPG, CPG2 and ceramide-phosphate (Fig. 6C). CCNA 01218 is annotated as a sphingosine kinase-related protein and has a conserved LCB5 domain (Nagiec et al., 1998). Therefore, we propose that CCNA 01218 adds the initial phosphate on the ceramide. Lastly, the $\triangle CCNA$ 01219 mutant lost CPG and CPG2 but retained ceramide-phosphate (**Fig. 6C**). This is consistent with CCNA 01219 adding a glycerate molecule to ceramide-phosphate to form CPG. CCNA 01219 has no conserved domains, and a BLAST analysis identified homologs only in Caulobacterales and Sphingomonodales. Each deletion could be complemented by expressing the respective gene from a vanillate-inducible promoter (Fig. 6C).

Based on these data, we propose a mechanism where CCNA_01218 (CpgB) phosphorylates ceramide, CCNA_01219 (CpgC) adds a glycerate, and CCNA_01217 (CpgA) adds a second phosphoglycerate (**Fig. 6D**). We note that the amount of CPG/CPG2 detected appears to be a relatively small percentage of the total lipidome (**Fig. S4**), raising the question of how these lipids can enable survival in the absence of lipid A. The CPG2 molecule is very

polar, as evidenced by its very long LC retention time, and we expect that this lipid is not efficiently extracted by standard methods. Though we tried several modifications to increase the extraction yield, we made only marginal improvements. Additionally, our genetic data show that CpgA adds the second phosphoglycerate molecule to generate CPG2, but we cannot rule out the possibility of higher-order polymers containing additional phosphoglycerates, which would be even more polar and difficult to extract.

Ceramide phosphoglycerate mediates susceptibility to colistin

Cationic antimicrobial peptides (CAMPs) have been demonstrated to kill Gram-negative bacteria by first interacting with negatively charged groups on surface-exposed LPS. Phosphates at the 1 and 4□ positions of lipid A are particularly important for this interaction, and several bacteria possess mechanisms to modify them, reducing their negative surface charge and sensitivity to CAMPs (Moffatt et al., 2019; Velkov et al., 2010). Despite lacking phosphate groups on its lipid A, *Caulobacter* is highly sensitive to colistin (**Fig. 7A**) and the antimicrobial effect is retained in the lipid A-deficient strain Δ*lpxC* Δ*fur* Δ*sspB* (**Fig. 7A**). Since the CPG/CPG2 lipids are anionic, we considered whether they may be the colistin target in *Caulobacter*. Indeed, the growth of mutants lacking *cpgA*, *cpgB*, or *cpgC* was unaffected by colistin (**Fig. 7A**). Since the deletion of *cpgA*, catalyzing the conversion of CPG to CPG2, can alone greatly reduce colistin sensitivity, and since the elimination of lipid A had no effect, we infer that a primary target of colistin on the *Caulobacter* surface is CPG2. Furthermore, these findings are consistent with our hypothesis that CPG lipids are a significant component of the OM whose detection is limited by inefficient extraction.

Discussion

CtpA is required for wild-type lipid A structure and abundance

We performed a suppressor screen to discover the essential function of CtpA, which contains active site residues characteristic of tyrosine phosphatases. Inactivation of *fur* or genes involved in O-antigen synthesis permitted the deletion of *ctpA* and yielded cells with drastically reduced amounts of lipid A. MS/MS analysis of the remaining lipid A extracted from $\Delta ctpA$ Δfur $\Delta sspB$ were consistent with species that retain phosphoryl groups at the 1 and 4 \square positions of the central disaccharide, suggesting that CtpA is responsible for dephosphorylating at least one of these positions, in preparation for the addition of GalpA residues.

Some alphaproteobacteria produce lipid A species with a tri- or tetrasaccharide backbone (De Castro et al., 2008). In *Rhizobia*, the phosphatases LpxE and LpxF

dephosphorylate the 1 and $4\Box$ positions, respectively, of lipid A at the periplasmic surface of the IM (Karbarz et al., 2003; Wang et al., 2006). Sugars are then added to the 1 and $4\Box$ positions by the glycosyltransferases RgtF and RgtD, respectively, before the transport of mature LPS molecules to the OM (Brown et al., 2012, 2013). NA1000 harbors a gene ($CCNA_03113$) with similarity to LpxE, but none with similarity to LpxF, raising the possibility that CtpA substitutes for LpxF. Additional work is required to verify this model; however, dephosphorylation of a lipid A intermediate by CtpA could explain the ability of mutations in O-antigen synthesis to suppress $\Delta ctpA$. If the retention of 1- and $4\Box$ -phosphates impairs lipid A trafficking, then removal or reduction of the O-antigen could partially compensate and allow at least a small amount of structurally altered lipid A to reach the cell surface.

The elimination of lipid A in Caulobacter crescentus requires a novel anionic sphingolipid

Here we demonstrate that the enzyme LpxC and lipid A itself are dispensable for viability in Caulobacter crescentus, conditional upon the absence of Fur and the presence of a previously uncharacterized anionic sphingolipid, ceramide phosphoglycerate (Fig. 7B). LPS molecules form a robust permeability barrier based on 1) tight packing of the six saturated acyl chains of lipid A, and 2) a lateral network formed by the bridging of phosphate groups on lipid A or the core polysaccharide by divalent cations such as Mg²⁺ and Ca²⁺ (Nikaido, 2003). Caulobacter lipid A and core polysaccharide lack the phosphates that would participate in a lateral network with divalent cations (Smit et al., 2008). We propose that negative charges on CPG/CPG2 can provide this function in the Caulobacter OM, accounting for the observation that cpgABC and other sphingolipid synthesis genes are important for fitness even in non-stress conditions (Fig. 5A and Christen et al., 2011). Evidence that CPG/CPG2 contribute negative charge to the Caulobacter OM comes from studies of CAMP sensitivity. We previously observed that Spt is necessary for susceptibility to polymyxin B, but Sgt1 and Sgt2, which convert neutral ceramide to the anionic glycosphingolipid GSL-2, are not required (Stankeviciute et al., 2019). This result was puzzling, because neutral ceramide was not expected to be a target for CAMP activity. Here we provide an explanation by showing that neutral ceramide is converted by CpgABC to a different anionic species, CPG2, and that this lipid, rather than LPS, is critical for colistin susceptibility.

Inhibition of Fur-mediated gene expression is necessary to survive in the absence of lipid A

In contrast to Sphingomonads, the presence of cell surface sphingolipids is not sufficient for Caulobacter to survive in the absence of lipid A. Instead, the iron-responsive transcription

factor Fur must also be deactivated. Both iron limitation (via growth in 2,2-dipyridyl) and excess available iron (due to a disruption in iron homeostasis in Δfur) supported the viability of lipid A-deficient *Caulobacter*. These results imply that genes or processes regulated by Fur in complex with iron, rather than those regulated by iron independently of Fur, are the critical factors.

Fur controls iron homeostasis in *Caulobacter* by directly or indirectly regulating ~120 genes in combination with iron (Leaden et al., 2018; da Silva Neto et al., 2009, 2013). A significant fraction of the Fur regulon, comprising 45 genes, is predicted to encode membrane proteins functioning in transport reactions or energy metabolism. *Caulobacter* Fur represses the transcription of genes predicted to mediate iron uptake, and it activates the expression of genes encoding iron-containing enzymes, including respiratory complexes containing Fe/S clusters or heme groups. Fur is linked to oxygen signaling in *Caulobacter* by activating the transcription of *fixK*, which mediates the response to hypoxia (Crosson et al., 2005). In addition, the Δfur mutant has a constitutively elevated level of intracellular oxidation, implicating Fur in the prevention of oxidative stress (Leaden et al., 2018).

Our *ctpA* suppressor screen retrieved mutations in *fur*, but not in genes whose transcription is activated by Fur. Thus, there is unlikely to be a singular Fur-regulated gene whose expression prevents the elimination of lipid A. Consistently, RB-Tnseq revealed that no transposon insertions in Fur-activated genes led to significantly increased fitness during challenge with CHIR-090. Since suppressor mutations would be more likely to cause loss than gain of function, we might not retrieve suppressors that work by increasing gene expression or activity. However, if there were a single Fur-repressed gene whose upregulation was critical for the ability to lose lipid A, then transposon insertions in this gene would be expected to reduce the fitness of CHIR-090-treated cells. Again, no individual gene fits this profile, but one caveat is that essential genes are excluded from RB-Tnseq analysis.

Based on our genetic data, mutations in *fur* could support the viability of lipid A-deficient *Caulobacter* via 1) downregulation of multiple Fur-activated genes, 2) upregulation of multiple Fur-repressed genes, and/or 3) activation of compensatory cellular stress responses. Since Fur regulates the expression of many OM and IM proteins, deletion of *fur* could alter envelope composition in a manner that renders lipid A non-essential. Alternatively, the transcriptional changes and oxidative stress which follow from *fur* deletion could activate a network of stress responses which together make it possible to eliminate lipid A.

The search for principles governing lipid A essentiality

Hypotheses to explain the essential nature of lipid A include its chemical barrier function, the detrimental activation of stress responses when it is depleted, its role in OM protein biogenesis or function, and its mechanical role in resisting turgor pressure (Rojas et al., 2018; Zhang et al., 2013). *Caulobacter* is only the fourth LPS-bearing Gram-negative bacterium demonstrated to survive in the absence of lipid A, following *N. meningitidis*, *M. catarrhalis*, and *A. baumannii*. So far, however, no single theme has emerged to explain why this select and phylogenetically diverse group of Gram-negative species is capable of surviving without lipid A.

In *A. baumannii*, proteins which synthesize PG in lateral cell walls (the elongasome) are critical for the fitness of lipid A-deficient strains, suggesting that alterations in PG structure are needed to compensate for the OM's loss of mechanical strength (Simpson et al., 2021). However, since elongasome components are essential for viability in wild-type *Caulobacter* (Christen et al., 2011), RB-Tnseq could not reveal their fitness effects in CHIR-090-treated cultures. Lipid A-deficient strains of *A. baumannii* consistently display increases in the expression of lipoproteins and the Lol pathway for lipoprotein transport to the OM (Boll et al., 2016; Henry et al., 2015). Two lipoprotein synthesis genes, *Igt* (*CCNA_00525*) and *Int* (*CCNA_00050*), had markedly reduced fitness scores in CHIR-090-treated *Caulobacter* cultures compared to unstressed cultures, so OM lipoproteins may help to compensate for the absence of lipid A in diverse species.

A. baumannii $\Delta lpxC$ mutants have growth and morphological defects that are corrected when the growth rate is limited by environmental factors such as low temperature or nutrient limitation (Nagy et al., 2019), suggesting that one barrier to the elimination of lipid A is the rate of synthesis of alternative molecules to constitute the OM. Although Δfur slows the growth of Caulobacter (Fig. S1, Table S3, and da Silva Neto et al., 2009), we found that slow growth in PYE medium at a reduced temperature was not sufficient to support the viability of fur^+ Caulobacter depleted of LpxC (Fig. S5A), or of $\Delta lpxC$ Δfur $\Delta sspB$ cells with fur expression restored (Fig. S5B). The Δfur mutation therefore provides a benefit beyond decreasing the growth rate, which remains to be elucidated.

Our work suggests that possession of genes to produce anionic sphingolipids may provide certain bacteria with a unique pathway to the elimination of lipid A. In addition to facilitating OM remodeling, anionic sphingolipids can also underlie clinically important phenotypes, even in wild-type membranes that retain LPS, such as the susceptibility to CAMPs, which are used as a last line of defense against multidrug-resistant bacterial infections. Thus, functions traditionally attributed to lipid A may be performed wholly or in part by alternative

lipids, underscoring the need to study lipid A functions in diverse species and to identify and functionally characterize novel lipids.

Acknowledgments

 The authors thank Charlie Huang, Morgan Price, Laura Herron and Henry Seaborn for experimental assistance. Cryoelectron microscopy data acquisition was performed using instrumentation of Lawrence Berkeley National Laboratory and the Bay Area CryoEM resource, maintained by Jonathan Remis and Daniel Toso respectively. Assistance in Linux computer maintenance was provided by Paul Tobias. D.R.G. thanks the International Centre for Cancer Vaccine Science project of the International Research Agendas program of the Foundation for Polish Science co-financed by the European Union under the European Regional Development Fund MAB/2017/03 at the University of Gdansk. Funding for this work was provided by National Science Foundation awards 1553004 and 2031948 to E.A.K. and 1615287 to K.R.R., and National Institutes of Health awards GM111066-01 and 1R01Al123820-01 to D.R.G. Cryoelectron tomography work was supported by the Laboratory Directed Research and Development Program of Lawrence Berkeley National Laboratory under U.S. Department of Energy Contract No. DE-AC02-05CH11231.

Author contributions

J.J.Z., E.A.K., and K.R.R. conceived the project. Mass spectrometry experiments were performed and analyzed by S.H.Y., D.R.G., and Z.G. Electron cryotomography experiments were performed and analyzed by R.G. and K.M.D. RB-Tnseq experiments, sequencing, and data analysis were performed by J.J.Z and A.M.D., and K.R.R. All other experiments were performed and analyzed by J.J.Z., G.S, E.A.K., and K.R.R. The manuscript was written by J.J.Z., E.A.K, and K.R.R. with input from all authors.

Declaration of interests

The authors declare no competing interests.

Figure Legends

- **Figure 1**. Suppressor mutations affecting *fur* or O-antigen biosynthesis permit the loss of *ctpA*.
- 567 (A) Strategy for isolation of Δ*ctpA* suppressor mutants. (B) Viability of suppressor strains during
- 568 CtpA depletion on PYED. (C) Differential interference contrast (DIC) images of the indicated

strains grown in CtpA-expressing (PYEX) or non-expressing (PYED) conditions. D) DIC images of the indicated strains grown to exponential phase in PYE. Scale bar, 3 µm.

Figure 2. ΔctpA and ΔlpxC strains with suppressor mutations contain little or no lipid A. (A) Endotoxin units (EU) per mL of whole cells of the strains indicated in panel B (mean ± S.D., N=3). Dots represent individual data points, and mean values are displayed above bars. (B) Hot aqueous-phenol LPS extracts of the indicated strains. *** = S-LPS, ** = putative full-length lipid A-core, * = putative lipid A. (C) Lipid A (left) or rough LPS (right) extracted from the indicated strains. * = lipid A. ** = rough LPS. (D) Proteinase K-treated lysates of the indicated strains. Cells were maintained in PYED or shifted into PYEX for 6 hours before harvesting. Samples were normalized by OD₆₆₀. NA1000 was grown in PYE. Leaky expression of LpxC can generate S-LPS (***) and lipid A + core (**) in PYED. Full-length S-LPS is not restored to ctpA and the lipid A-core species is reduced in size (*) because CCNA_03733 is needed for mannose incorporation. (E) Electron cryotomography images of the indicated strains noting the inner membrane (IM), peptidoglycan (PG), outer membrane (OM), and S-layer. All strains were grown to exponential phase in PYE medium, except that CtpA was depleted from KR3906 during 12 hours of growth in PYED prior to analysis. Scale bars, 100 nm.

Figure 3. Deletion of *fur* supports the viability of $\Delta lpxC$ cells. (A) DIC images of the LpxC depletion strain alone or harboring the indicated mutations, grown in PYEX or PYED for 10 hours. Scale bar, 3 µm. (B) Viability of the LpxC depletion strain, alone or harboring the indicated mutations, plated on PYEX or PYED. (C) Viability of $\Delta lpxC$ Δfur $\Delta sspB$ cells harboring a Pxyl-*fur* or a Pxyl-*cerulean* expression vector. Plates included kanamycin to retain expression vectors.

Figure 4. Fur-regulated processes control the conditional essentiality of lipid A. (A) Sensitivity to the indicated chemicals measured by disc diffusion assay. Dots indicate individual data points. Suppressor mutations present in strains represented by blue or green bars are, from left to right, $\Delta CCNA_00497$, $\Delta CCNA_01553$, $\Delta CCNA_03733$, and Δfur . (B) CHIR-090 sensitivity measured by disc diffusion assay. Partial clearing indicates the diameter of a ring of intermediate growth. Dots and triangles indicate individual measurements of cleared and partially cleared zones, respectively (mean ± S.D., N=3). (C) Viability of the LpxC depletion strain in inducing (PYEX) or depleting (PYED) conditions, in the presence or absence of 100 μM 2,2'-dipyridyl. (D) Viability of the Δ*lpxC* Δ*fur* Δ*sspB* strain harboring a Pxyl-*fur* plasmid, grown in noninducing (PYED) or

inducing (PYEX) conditions, in the presence or absence of 100 μ M 2,2'-dipyridyl. Plates included kanamycin to retain the expression vector. Brightness was reduced and contrast increased to improve the clarity of colonies grown on 2,2'-dipyridyl. (E) Proteinase K-treated lysates of the indicated strains grown overnight in the presence or absence of 100 μ M 2,2'-dipyridyl. Samples were normalized by OD₆₆₀. (F) Growth inhibition by SNG in liquid PYE cultures of the indicated strains. Dots represent individual OD₆₆₀ ratios (mean \pm S.D.). (G) Genes regulated by Fur in concert with iron (sets A and B) are modulated similarly by deletion of *fur* or by iron limitation, while genes regulated by iron alone (sets C and D) are modulated in opposite directions. Changes in Fur-regulated gene expression correlate with the ability to lose lipid A.

Figure 5. RB-Tnseq identifies sphingolipid synthesis genes needed for fitness when LpxC is inhibited. (A) Average gene fitness scores for three challenges of the NA1000 RB-Tnseq library with PYE or PYE+2 μg/ml CHIR-090. Fitness scores are color-coded based on regulation of the corresponding genes. Fitness scores of selected genes (not regulated by Fur or iron) are indicated by colors matching the open reading frame diagram below. (B) CHIR-090 sensitivity of the indicated strains measured by disc diffusion assay (mean ± S.D.) Where indicated, 0.5 mM vanillate was included in the medium. (C) Overnight growth of strains expressing (xylose) or depleting (dextrose) LpxC, and expressing (vanillate) or not expressing the indicated genes. Dots represent individual measurements (mean ± S.D.).

Figure 6. *CCNA_01217-01219* convert neutral ceramide to an anionic sphingolipid, ceramide phosphoglycerate. (A) Extracted ion-chromatograms identified the indicated sphingolipid species in NA1000 lipid extracts. (B) Structural determination of anionic sphingolipids was performed by MS/MS analysis. (C) The presence of the indicated sphingolipids was assessed in each deletion mutant and its respective complemented strain. x, no lipid of that type was detected in the indicated strain. (D) Proposed mechanism for CPG2 synthesis.

Figure 7. Ceramide phosphoglycerate mediates susceptibility to colistin. (A) Overnight growth of the indicated strains in the presence or absence of 10 µg/ml colistin. Dots represent individual OD₆₆₀ measurements (mean \pm S.D.). (B) Model of the *Caulobacter* cell envelope containing LPS and CPG2. Consequences for OM composition and colistin sensitivity when either lipid A ($\Delta lpxC$ Δfur) or sphingolipids (Δspt) are eliminated. The presence of CPG2 and the absence of *fur* are together required for the viability of lipid A-deficient *Caulobacter*.

637 638 639 640 Methods 641 Growth conditions. All Caulobacter crescentus strains were derived from NA1000 (Evinger 642 and Agabian, 1977) and are listed in Table S4. Unless otherwise stated, Caulobacter was 643 grown in peptone-yeast extract medium (PYE) (Ely, 1991) at 30°C. Solid media were prepared 644 using Fisher agar (BP1423). PYE was supplemented with 0.3% xylose (PYEX) or 0.2% D-645 glucose (PYED) where indicated. When changing between inducing and non-inducing 646 conditions, cells were washed twice with PYE medium lacking additional sugars before being 647 released into or plated on medium supplemented with a different sugar. Counter-selection using 648 sacB was performed using 3% sucrose. 100 µM 2.2'-dipyridyl was added to culture media to 649 achieve low-iron conditions. Vanillic acid was added to PYE media at a final concentration of 0.5 650 mM to drive gene expression from the vanA promoter. Antibiotics added to PYE were used at 651 the following concentrations (µg/mL) for liquid (L) or solid (S) medium: kanamycin, 5 (L), 25 (S); 652 chloramphenicol, 1 (L/S); nalidixic acid, 20 (S); gentamycin, 25 (L), 5 (S); oxytetracycline, 1 (L), 653 2 (S); spectinomycin, 25 (L), 100 (S); hygromycin, 100 (L/S); streptonigrin 0.025 or 0.25 (L). E. 654 coli was grown in lysogeny broth (10 g/L tryptone, 5 g/L yeast extract, 5 g/L NaCl) at 37°C, 655 supplemented with antibiotics at the following concentrations (µg/mL) for liquid (L) or solid (S) 656 medium: kanamycin, 30 (L), 50 (S); chloramphenicol, 20 (L), 30 (S); gentamycin, 15 (L), 20 (S); 657 tetracycline, 12 (L/S); spectinomycin, 50 (L/S); hygromycin, 100 (L/S). Diaminopimelic acid (0.3 658 mM) was added to solid or media to support the growth of E. coli strain WM3064 (Dehio and 659 Meyer, 1997). 660 661 Plasmid construction. Plasmid descriptions are listed in Table S5. Primer sequences used for 662 plasmid construction are listed in Table S6. 663 664 pZIK133. The LpxC depletion vector was constructed by placing the lpxC coding region, C-665 terminally fused to a 3xFLAG tag (amino acid sequence: DYKDHDGDYKDHDIDYKDDDDK) 666 followed by the Caulobacter ssrA tag (amino acid sequence: AANDNFAEEFAVAA), under 667 control of the xylX promoter. The xylX promoter was amplified using the pJS14-PxylX and 668 PxyIX-lpxC R primers. The PxyIX-lpxC F and lpxC-3xFLAG R primers were used to amplify 669 lpxC. The C-terminal fusion was amplified from pAB6 using the lpxC-3xFLAG F and ssrA-pJS14

671

672673

674

675

676

677

678

679

680 681

682

683

684

685

686

687

688

689

690 691

692

693

694

695

696

697

698

699

700

701

702

primers. The final plasmid was assembled via Gibson cloning into a BamHI/EcoRI-digested pJS14 backbone. pZIK134. For the IpxC knockout construct, flanking homology regions were amplified using the primers IpxC UpF and IpxC UpR for the 5'- region, and IpxC DownF and IpxC DownR for the 3'region. The 5'- arm included a 5'- Spel site and a 3'- EcoRI site, and the 3'- arm included a 5'-EcoRI site and a 3'- SphI site. These fragments were digested with the indicated enzymes and ligated into Spel/Sphl-digested pNPTS138. This intermediate plasmid was linearized with EcoRI, and the EcoRI-digested tetAR cassette from pKOC3 was inserted to make the final construct. pZIK73 and pZIK78. For knockouts of CCNA 01553 or CCNA 00497, flanking homology regions were amplified using the following primer pairs: pZIK73 5'- region (01553 UpF; 01553 UpR), pZIK73 3'- region (01553 DownF; 01553 DownR), pZIK78 5'- region (00497::hyg UpF; 00497::hyg UpR), pZIK78 3'- region (00497::hyg DownF; 00497::hyg DownR). For each construct, the 5'- arm included a 5'- Spel site and a 3'- Smal site, and the 3'- arm included a 5'-Smal site and a 3'- EcoRI site. These fragments were digested with the indicated enzymes and ligated into Spel/EcoRI-digested pNPTS138. The intermediate plasmids were linearized with Smal, and the Smal-digested hyg cassette from pHP45Ω-hyg was inserted to make the final constructs. pZIK80, pZIK81, pZIK82, and pZIK161. For the knockouts of CCNA 03733, CCNA 01068, CCNA 01055, or CCNA 00055, flanking homology regions were amplified using the following primer pairs: pZIK80 5'- region (03733::hyg UpF; 03733::hyg UpR), pZIK80 3'- region (03733::hyg DownF; 03733::hyg DownR), pZIK81 5'- region (01068::hyg UpF; 01068::hyg UpR), pZIK81 3'- region (01068::hyg DownF; 01068::hyg DownR), pZIK82 5'- region (01055::hyg UpF; 01055::hyg UpR), pZIK82 3'- region (01055::hyg DownF; 01055::hyg DownR), pZIK161 5'region (fur UpF; fur UpR), pZIK161 3'- region (fur DownF; fur DownR). Each 5'- arm included a 5'- Spel site and a 3'- BamHI site, and each 3'- arm included a 5'- BamHI site and a 3'- EcoRI site. These fragments were digested with the indicated enzymes and ligated into Spel/EcoRIdigested pNPTS138. The intermediate plasmids were linearized with BamHI, and the BamHIdigested hyg cassette from pHP45 Ω -hyg was inserted to make the final constructs.

- 703 pZIK172-174. CCNA 00497, CCNA 01553, or CCNA 03733 were placed under control of the
- 704 *xylX* promoter on pXCERN-2, which integrates at the *xylX* promoter. The corresponding genes
- were initially cloned into pVCERN-2 before being moved into pXCERN-2. Genes were amplified
- with the following primer pairs: CCNA 00497 (pVCERN-2 00497 F; pVCERN-2 00497 R),
- 707 CCNA 01553 (pVCERN-2 01553 F; pVCERN-2 01553 R), CCNA 03733 (pVCERN-2 03733 F;
- 708 pVCERN-2 03733 R). Primer sets replace the start codon with an Ndel site and add a Sacl site
- after the stop codon. The corresponding gene fragment and pVCERN-2 were digested with
- 710 Ndel and Sacl and ligated together. An Ndel/Mlul fragment was subsequently excised from
- 711 each vector and moved to pXCERN-2 cut with the same enzymes.
- 713 pZIK175. CCNA 00055 (fur) was placed under control of the xylX promoter on pXCERN-2,
- which integrates at the xylX promoter. CCNA 00055 was initially cloned into pVCERN-2 before
- being moved into pXCERN-2. CCNA_00055 was amplified using the Pvan-fur and fur-pVCERN
- 716 primers, and this fragment was inserted into Ndel/Sacl-digested pVCERN-2 via Gibson
- 717 assembly. The Ndel/Mlul fragment was subsequently excised and ligated into Ndel/Mlul-
- 718 digested pXCERN-2.
- 720 pGS74 and pGS76. For markerless deletions of CCNA 01217 or CCNA 01219, 5□- and 3□-
- 721 flanking homology regions, respectively, were amplified using the primer pairs EK1047/1048
- 722 and EK1049/1050 (CCNA 01217) and EK1055/1056 and EK1057/1058 (CCNA 01219).
- 723 pNPTS138 was amplified with primers EK897/898, and vectors were constructed by Gibson
- 724 assembly.

719

725

730

- 726 pKR429. For markerless deletion of CCNA 01218, 5 and 3 flanking homology regions,
- 727 respectively, were amplified using the primer pairs 01218 up fwd/01218 up rev and 01218
- down fwd/01218 down rev. pNPTS138 was digested with EcoRI and HindIII, and the vector was
- 729 constructed by Gibson assembly.
- 731 pEK406. For complementing the deletion of CCNA 01217 in LC-MS/MS experiments,
- 732 CCNA 01217-FLAG was amplified using primers EK1357/1358. The PCR product was ligated
- 733 into the Ndel/Nhel sites of pVCHYC-5.
- 735 pKR432-4. For appending a C-terminal FLAG tag to the CCNA 01218-20 open reading frames.
- 736 The indicated genes were amplified from NA1000 genomic DNA using primer pairs Nde-

737 01218/01218-Mlu, Nde-01219/01219-Mlu, Nde-01220/01220-Mlu. Fragments were digested

- vsing Ndel/Mlul and ligated into pFLGC-1 digested with the same enzymes.
- 740 *pKR435.* For expressing *CCNA_01218-FLAG* from the chromosomal vanA promoter.
- 741 CCNA 01218-FLAG was amplified from pKR432 using primers 01218-FLAG F/01218-FLAG R
- and inserted in Ndel-digested pVGFPC-2 by Gibson assembly.
- 744 pKR436. For expressing CCNA 01219-FLAG from the chromosomal vanA promoter.
- 745 CCNA_01219-FLAG was amplified from pKR433 using primers 01219-FLAG F/01219-FLAG R
- and inserted in Ndel-digested pVGFPC-2 by Gibson assembly.
- 748 pKR437. For expressing CCNA 01220-FLAG from the chromosomal vanA promoter.
- 749 CCNA 01220-FLAG was amplified from pKR434 using primers 01220-FLAG F/01220-FLAG R
- and inserted in Ndel-digested pVGFPC-2 by Gibson assembly.
- 752 *pKR438*. For expressing *CCNA_01217-FLAG* from the chromosomal vanA promoter.
- 753 CCNA_01217-FLAG was amplified from pEK406 using primers 01217-FLAG F/01217-FLAG R
- and inserted in Ndel-digested pVGFPC-4 by Gibson assembly.
- 756 **Strain construction**. Unless otherwise stated, plasmids were mobilized from *E. coli* into *C.*
- 757 crescentus by conjugation. E. coli donors were counterselected by the addition of nalidixic acid,
- or when WM3064 was used as the donor, by omitting diaminopimelic acid from selection plates.
- 759 Gene deletion or disruption was achieved by two-step homologous recombination using sacB
- 760 counterselection (Ely, 1991).

739

743

747

751

755

- 762 CtpA depletion strain. In the CtpA depletion strain (KR3906, Shapland et al., 2011), regulated
- depletion of CtpA is achieved by expressing ctpA::3xFLAG::ssrA from a xylose-inducible
- promoter (Meisenzahl et al., 1997) on a high-copy plasmid in a $\Delta ctpA$ strain also lacking the
- 765 proteolytic adaptor sspB (Levchenko et al., 2000). The native CtpA protein could not be
- depleted without an ssrA tag to target it for proteolysis. However, addition of this tag made CtpA
- proteolysis so rapid that xylose-dependent expression of CtpA-3xFLAG-ssrA did not support
- 768 Caulobacter viability. Further deleting sspB, which encodes a proteolytic adaptor for ssrA-
- tagged substrates, reduced the basal rate of CtpA-3xFLAG-ssrA degradation enough to permit
- 770 complementation in PYE medium containing xylose (PYEX).

773

774

775

776

777

778779

780

781

782 783

784

785

786

787

788

789

790 791

792

793

794

795

796

797

798

799

800

801

802

803 804 LpxC depletion strain. The LpxC depletion strain KR4007 was constructed in a parallel manner to the CtpA depletion strain KR3906. pZIK133 was introduced to KR1499 (ΔsspB) by conjugation and selection on PYE/chloramphenicol, pZIK134 was conjugated into this intermediate strain, and colonies were selected on PYEX/chloramphenicol/oxytetracycline. After sacB counterselection on PYEX/sucrose/oxytetracycline, colonies were screened for chloramphenicol^R kanamycin^S on PYEX. Stable $\triangle ctpA$ or $\triangle lpxC$ strains. To generate stable $\triangle ctpA$ or $\triangle lpxC$ strains without covering plasmids, candidate suppressor genes identified by screening were disrupted in KR3906 or KR4007, respectively, using two-step homologous recombination while cultivating the cells on PYEX. Intermediate strains (sucrose^R hygromycin^R kanamycin^S) were grown in liquid PYED without chloramphenical to permit loss of the ctpA or lpxC covering plasmid, plated on PYED, and tested for chloramphenicol^s. Absence of *ctpA* was confirmed using primers ctpA KO F and ctpA KO R, and absence of IpxC was confirmed using primers IpxC KO F and IpxC KO R. The genomes of $\Delta ctpA$ Δfur $\Delta sspB$ (KR4102) and $\Delta lpxC$ Δfur $\Delta sspB$ (KR4103) were resequenced and contained no additional mutations. Stable $\Delta ctpA$ or $\Delta lpxC$ strains were further modified by electroporation with purified plasmids (Gilchrist and Smit, 1991) to restore xylose-driven suppressor gene expression. Unmarked deletions in genes for ceramide phosphoglycerate synthesis. Deletions in CCNA 01217, CCNA 01218, CCNA 01219, and CCNA 01220 in NA1000 or KR4077 were made by conjugation of the appropriate pNPTS138-based plasmid, followed by selection on PYE/kanamycin/nalidixic acid. After overnight growth in PYE, cells were plated on PYEX/sucrose, and sucrose^R colonies were screened for kanamycin^S. Colony PCR with the following primers was used to detect the deletion of the indicated chromosomal genes: CCNA 01217, EK S238/S239; CCNA 01218, EK S240/S241; CCNA 01219, EK S242/S243; CCNA 01220, EK S216/S217. Loci were sequenced with the indicated primers to ensure the accuracy of in-frame deletions. Unmarked deletions of CCNA 01217, CCNA 01218, CCNA 01219, and CCNA 01220 were made in KR4091 by conjugation of KR4091 with WM3064 harboring the appropriate pNPTS138-based plasmids, followed by selection on PYEX/kanamycin medium omitting diaminopimelic acid. After growth overnight in PYEX, cells were plated on PYEX/sucrose, and sucrose^R colonies were screened for kanamycin^S. Colony PCR with the following primers was used to detect the deletion of the indicated chromosomal

806

807

808 809 810

811

812

813

814

815

816

817

818

819820

821

822

823

824

825

826

827

828829

830

831

832

833

834

835

836

837

838

genes: CCNA 01217, EK S238/S239; CCNA 01218, EK S240/S241; CCNA 01219, EK S242/S243; CCNA 01220, EK S216/S217. Loci were sequenced with the indicated primers to ensure the accuracy of in-frame deletions. Strains were screened for oxytetracycline and hydromycin^R to ensure that they maintained deletions of *lpxC* and *fur*, respectively. Complementation of genes for ceramide phosphoglycerate synthesis. To complement deletions of CCNA 01217-01220, the following plasmids were introduced by conjugation to place the complementing gene under control of the chromosomal *vanA* promoter: ΔCCNA 01217. pEK406 (for LC-MS studies) or pKR438 (for growth and chemical sensitivity assays); ΔCCNA 01218, pKR435; ΔCCNA 01219, pKR436; or ΔCCNA 01220, pKR437. When introducing plasmids into strains capable of IpxC depletion (based on KR4091), plasmids were delivered from WM3064 to avoid the use of multiple antibiotics for selection/counterselection. Correct integration of plasmids at the vanA locus was confirmed by colony PCR using primers RecUni-1 and RecVan-2 (Thanbichler et al., 2007). Suppressor selection. KR3906 was grown to full density in PYEX. 300 µL of culture was transferred onto an open, sterile Petri dish and mutagenized in a UV Stratalinker 1800 (Stratagene) with 30,000 µJ of energy. Mutagenized cells were plated on PYED. Recovered colonies were passaged in liquid PYED overnight to allow loss of the covering plasmid, and samples were streaked onto PYED. Isolated colonies were screened for chloramphenicol sensitivity. Chlor^S isolates were grown in PYE and saved at -80°C in 10% dimethylsulfoxide. Loss of ctpA was confirmed via PCR using the primers ctpA KO F and ctpA KO R, which anneal to the interior of the open reading frame. Genome resequencing. Strains were grown to full density in PYE, and genomic DNA was extracted using the Quick-DNA Miniprep Kit (Genesee) or the DNeasy Blood & Tissue Kit (Qiagen). Genomic DNA was submitted to the UC Berkeley Functional Genomics Laboratory, where libraries were prepared using a PCR-free protocol with multiplexing (http://gb3.berkeley.edu/gsl/). Samples were sequenced at the UC Berkeley Vincent J. Coates Genomics Sequencing Laboratory using a 300PE or 150PE MiSeq v3 run. Genomic sequencing data were analyzed for variants using the Galaxy platform at usegalaxy.org (Afgan et al., 2016). Adapter sequences were removed using Cutadapt, and sequences were aligned to the NA1000 genome (Marks et al., 2010) using Bowtie2. FreeBayes was used to analyze the BAM files for variants. Variants with quality scores below 300 were discarded as noise.

841

842

843

844

845

846

847

848849

850

851

852

853

854

855

856

857

858

859 860

861

862

863

864

865

866 867

868

869

870

871

872

Growth and viability assays. For plate assays, strains were grown to OD₆₆₀ = 0.2-0.5 in permissive media, washed twice in PYE medium with no additions, and diluted to $OD_{660} = 0.1$. 10 µl drops of ten-fold serial dilutions were pipetted onto permissive and nonpermissive media. Plates were incubated for 3 days at 30°C, and images are representative of at least three independent trials. For end-point growth assays in liquid media, strains were grown in permissive media to OD₆₆₀ = 0.2-0.5. After washing in PYE medium without additions, cells were resuspended at OD₆₆₀ = 0.01 in permissive and nonpermissive media. OD₆₆₀ values were measured after 24 h growth at 30°C. Disc diffusion assays of chemical sensitivity. Cultures were grown to mid-exponential phase $(OD_{660} 0.2-0.5)$, and an amount of cells equivalent to 250 μ l of culture at $OD_{660} = 0.2$ was added to 4 ml of PYE swarm agar (0.3% w/v agar) pre-warmed to 42°C. Swarm agar containing bacteria was spread onto solid PYE and allowed to set. Antibiotics or detergents (10 µl each) were added to sterile Whatman filter disks and allowed to dry in a fume hood before discs were placed onto swarm agar surfaces. Plates were incubated upright at 30°C for 24 hours. The diameters of the zones of clearing or haze were measured, and the diameter of the disk (6 mm) was subtracted from all measurements to yield the reported values. The total amount of antibiotic or detergent added to each disk is as follows: kanamycin (100 µg), rifampicin (100 µg). vancomycin (1 mg), CHIR-090 (100 μg, APExBIO), bacitracin (50 μg), TWEEN 20 (10 μL of 10% solution), Triton X-100 (10 μ L of 10% solution), sodium dodecyl sulfate (10 μ L of 10% solution). Tests using CHIR-090 used one quarter of the standard amount of cells to reduce growth haze. For strains overexpressing genes integrated at the vanA locus, uninduced cells were grown in PYE/kanamycin or PYE/gentamicin, and aliquots were plated in PYE swarm agar on PYE medium. Induced cells were grown in PYE/kanamycin or PYE/gentamicin containing 0.5 mM vanillate before plating in/on PYE medium containing 0.5 mM vanillate. 100 µM 2,2'dipyridyl was included in media for testing chemical sensitivity in iron-restricted conditions. Streptonigrin sensitivity. Isolated colonies of the indicated strains were grown in PYE medium to $OD_{660} = 0.2-0.5$ and diluted to $OD_{660} = 0.01$. The diluted culture was aliquoted into separate tubes, which received 0.025 µg/ml, 0.25 µg/ml, or no streptonigrin (SNG). After 24 h of growth at 30°C, OD₆₆₀ values were measured, and optical density ratios (0.25 µg/ml SNG/no addition and 0.025 µg/ml SNG/no addition) were calculated as a measure of growth inhibition.

Limulus amebocyte lysate (LAL) assay. The ToxinSensor Chromogenic LAL Endotoxin Assay kit (GenScript) was used to determine endotoxin units/mL of culture. Cells were grown to mid-exponential phase (OD₆₆₀ 0.2-0.5), washed twice with non-pyrogenic LAL reagent water, and normalized in this water to OD₆₆₀ = 0.1. Cell suspensions were serially diluted in non-pyrogenic water and analyzed according to manufacturer's instructions.

Extraction and visualization of LPS and lipid A species. For visualizing LPS species from whole-cell lysates, cells were harvested after overnight growth in the indicated medium. All cultures were normalized by OD₆₆₀, pelleted, and resuspended to 100 μL in 1x tricine loading buffer (100 mM Tris-HCl pH 6.8, 1% sodium dodecyl sulfate (SDS), 20% glycerol, 0.02% Coomassie G-250, 1% 2-mercaptoethanol). Proteinase K (125 ng/μL) was added, and samples were incubated overnight at 55°C. Lysates were boiled 5 min, and equal volumes (10% of each sample) were analyzed by gel electrophoresis.

Hot aqueous-phenol LPS extractions were adapted from Westpahl and Jann (Davis and Goldberg, 2012; Westphal and Jann, 1965). 1 mL of culture at OD_{660} = 0.75 was pelleted and resuspended in 200 µL 1x tricine loading buffer. Suspensions were boiled for 15 min and cooled to room temperature. 5 µL of 20 mg/mL Proteinase K (Thermo) was added to each sample before incubation at 55°C for three hours. Suspensions were mixed with 200 µL ice-cold Trissaturated phenol, vortexed, and incubated at 65°C for 15 minutes before being cooled to room temperature. 1 mL diethyl ether was added to each sample before vortexing and spinning for 10 minutes in a table-top centrifuge at 16,000 x g. The bottom blue layer was removed to a fresh tube, and the extraction was repeated on the blue layer starting from the phenol step. 200 µL 2x tricine loading buffer was added to each sample before gel electrophoresis.

Rough LPS was extracted by the method of Darveau and Hancock (Darveau and Hancock, 1983), modified as described (Hershey et al., 2019), beginning with 50 ml PYE cultures grown to OD_{660} = 0.85. Cultures were centrifuged, and cell pellets were resuspended in 2 ml 10 mM Tris-HCl (pH 8.0) containing 2 mM MgCl₂. Samples were sonicated (Qsonica Q500) on ice for 5 min at 20% amplitude, in cycles of 10 sec on/20 sec off so that fewer than 5% of cells remained intact. DNase I and RNase A were added to final concentrations of 100 µg/ml and 25 µg/ml, respectively, and lysates were incubated at 37°C for 1 hour. Additional DNase I and RNase A were added to reach final concentrations of 200 µg/ml and 50 µg/ml, respectively, and lysates were incubated for 1 hour at 37°C. SDS and EDTA were added to achieve final concentrations of 2% and 100 mM, respectively, and lysates were incubated for 2 h at 37°C before centrifugation (30 min at 50,000 x g, 30 min, 4°C). Proteinase K (50 µg/ml) was added to

each supernatant, followed by incubation for 2 h at 60° C. LPS was precipitated by the addition of 2 volumes of ice-cold 0.375 M MgCl₂/95% ethanol and collected by centrifugation (12,000 x g, 15 min, 4°C). Precipitates were resuspended in 3.3 ml 10 mM Tris-HCl (pH8.0)/2% SDS/100 mM EDTA and incubated with shaking overnight at 37°C. Rough LPS was reprecipitated using 2 volumes ice-cold 0.375 M MgCl₂/95% ethanol and collected by centrifugation (12,000 x g, 15 min, 4°C). Precipitates were suspended in 10 mM Tris-HCl (pH 8.0) and centrifuged (200,000 x g, 2 h, 4°C). After removal of the supernatant by pipetting, LPS pellets were resuspended in 1 mll 1x tricine loading buffer, and 5 µl were analyzed by gel electrophoresis.

Free lipid A was extracted by the Caroff method (El Hamidi et al., 2005), modified as described (Leung et al., 2017), starting with 10 ml of PYE culture grown to OD₆₀₀ = 0.6. Cultures were divided into multiple tubes and centrifuged at 14,000 x g for 2 min. In a fume hood, cell pellets from each culture were resuspended, combined, and transferred to a gasketed microcentrifuge tube using 250 µl 70% (v/v) isobutyric acid + 150 µl 1 M ammonium hydroxide. Samples were incubated in a boiling water bath in a fume hood for 1 h, with vortexing every 15 min. Samples were cooled on ice and centrifuged at 2000 x g for 15 min. In a fume hood, supernatants (~400 µl) were transferred to new gasketed tubes, each containing 400 µl endotoxin-free water. Small holes were punched in the gasketed caps using a syringe needle before the samples were frozen in liquid nitrogen and lyophilized overnight. Methanol (1 ml) was added, and samples were sonicated in a water bath for 5 min. Samples were centrifuged at 10,000 x g for 5 min, and methanol was aspirated. The methanol wash was repeated before lipids were solubilized in 190 µl 3:1.5:0.25 v/v/v chloroform:methanol:endotoxin-free water. After vortexing, samples were centrifuged at 8,000 x g for 5 min. Supernatants were transferred to fresh gasketed tubes, and extracts were dried under a stream of nitrogen before analysis by mass spectrometry (see below) or gel electrophoresis. Samples for gel electrophoresis were resuspended using 100 µl 1x tricine loading buffer, and 10 µl of each sample was analyzed.

All lipid samples were analyzed on 16.5% Mini-PROTEAN Tris-Tricine gels (Bio-Rad). Carbohydrates were stained using Pro-Q Emerald 300 Lipopolysaccharide Gel Stain Kit (Molecular Probes; P20495) per manufacturer's instructions. For Western blot analysis of S-LPS, equal numbers of cells grown in PYE with appropriate additions were pelleted, resuspended in 1x SDS loading buffer, and boiled before analysis on 12% polyacrylamide gels and transfer to Immobilon-P PVDF membranes. Blots were probed with α-S-LPS (1:20,000) (Walker et al., 1994) and horseradish peroxidase-conjugated anti-rabbit antibodies (1:5000) and analyzed using Western Lightning. Stained lipid species were visualized using a Bio-Rad Gel Doc XR.

942

943

944

945

946

947

948

949

950

951

952

953

954

955

956

957

958

959

960

961

962963

964

965

966

967

968

969

970

971

972

973

974

High performance liquid chromatography-tandem mass spectrometry (HPLC-MSMS) of lipid A extracts. All samples for HPLC-electrospray ionization tandem mass spectrometry were generated by the modified Caroff extraction protocol described above. Each extract was initially dissolved in 100 µL 1:2 chloroform: methanol before dilution 1:10 with methanol for analysis. A 2-5 µL aliquot of each solution was injected onto a Phenomenex Jupiter C4 column (2 x 50 mm, 5 μm, 300 Å) for HPLC-MSMS analysis with a Waters Acquity UPLC system coupled to a Thermo LTQ-Orbitrap Velos Pro mass spectrometer, which was equipped with an atmospheric pressure electrospray ionization source. For lipid detection, the HPLC-MSMS analyses were carried out with full-mass detection over a mass range of m/z 250 to 2000 in the Fourier transform MS mode, with negative-ion detection. The mass resolution was 60,000 FWHM @ m/z 400. Fragmentation product ion masses of the three most intense precursor ions were measured in the ion trap or orbitrap (7500 resolution) mass analyzer using stepped collisioninduced dissociation (35% of the normalized collision energy) or Higher energy collision-induced dissociation (35% of the normalized collision energy) activation energies. During data acquisitions, real-time mass calibration was applied with m/z 283.26454 as the lock mass for negative-ion detection. The mobile phase for separation was (A) 1 mM ammonium acetate solution and (B) 90% (1:1 acetonitrile/propanol)/10% water/1 mM ammonium acetate as the binary solvents for the 16-minute gradient elution: 0 to 10 min, 30% to 100%B; 10 to 12 min, 100% B and 12 to 12.1 min at 30% B, followed by column equilibration at 30% B from 12.1 to 16 min. The column flow rate was 0.35 mL/min and the column temperature was maintained at 40°C.

Lipid A structure analysis. MALDI-TOF MS was used to screen lipid extracts. To check structures, tandem MS and ancillary separation techniques were required. These are described below. HPLC-MSMS (above) describes the generation of data for structure determinations in Fig. S3. Notably, the triple deletion strain $\Delta ctpA$ Δfur $\Delta sspB$ contained no lipid A with sugars at the terminal (1 and 4') positions but rather contained phosphates, as found in canonical lipid A structures. The $\Delta lpxC$ Δfur $\Delta sspB$ strain contained an ion at 1412 m/z, the structure of which remains unclear. The HPLC-MSMS data of this ion showed no loss of phosphate, as seen in $\Delta ctpA$ Δfur $\Delta sspB$, nor loss of sugars, as seen for the NA1000, $\Delta sspB$, or Δfur $\Delta sspB$ strains. The fragmentation pattern strongly suggested that something other than lipid A was responsible for the ion at 1412 m/z. Given that cardiolipin is a common microbial membrane lipid, we carried out HILIC-MS (described below) with cardiolipin and lipid A standards. Both standards were retained by HILIC, as expected for hydrophobic molecules, but extracts from the $\Delta lpxC$ Δfur

ΔsspB mutant showed no ions at all, suggesting that the species at 1412 m/z is not hydrophobic enough to be retained. Regrettably, there remains no structure identified for the ion at 1412 m/z. Generally, structure analysis was conducted manually according to our prior effort in this field (Yoon et al., 2016).

Hydrophobic interaction liquid chromatography-mass spectrometry (HILIC-MS). A 10-μL aliquot of each solution was injected into a Waters Atlantis HILIC column (4.6 mm x 150 mm, 5 μm) to run LC-MS on a Water Acquity UPLC system coupled to a Thermo LTQ-Orbitrap Velos Pro mass spectrometer, which was equipped with an atmospheric pressure electrospray ionization source. For lipid detection, the HILIC-MS runs were carried out with full-mass detection over a mass range of *m/z* 80 to 2000 in the Fourier transform MS mode, with positive-ion and negative-ion detection, respectively, in two rounds of LC injections. The mass resolution was 60,000 FWHM @ *m/z* 400. During data acquisitions, real-time mass calibration was applied with *m/z* 391.28426 as the lock mass for positive-ion detection and with *m/z* 112.98563 as the lock mass for negative-ion detection. The mobile phase of HILIC was (A) 20 mM ammonium acetate solution (pH adjusted to 4.0 with acetic acid) and (B) methanol as the binary solvents for gradient elution: 0-4 min, 99% B; 4 to 12.5 min, 99% to 20% B and 12.5 to 15 min at 20% B, followed by column equilibration at 99% B for 5 min between injections. The column flow rate was 0.4 mL/min and the column temperature was maintained at 40°C.

Differential interference contrast microscopy. Cells were immobilized on agarose pads (1% w/v in reverse osmosis-purified water). Images were taken using a Zeiss EC Plan-Neofluar 100x/1.3 Oil M27 objective on a Zeiss AxioImager M1 microscope with a Hamamatsu Digital CCD Camera (C8484-03G01). Images were acquired using iVision software and processed using ImageJ.

CryoEM imaging and tomographic processing. Cultures (5 mL) of KR4000, KR4102, KR4103, and KR3906 grown to OD_{660} 0.2-0.5 were centrifuged (4°C, 16,000 x g, 15 minutes), and cell pellets were resuspended in 50 μ L PYE. For KR3906, cells grown in PYEX were washed twice with PYE, released into PYED at OD_{660} = 0.02, and incubated for 12 hours before harvest. 3 μ L of cell suspension, mixed 1:1 with Fiducial markers (10-nm gold particles conjugated to Protein A; Aurion) was applied to glow-discharged quantifoil grids (R2/2) and frozen in liquid ethane using an automatic plunge freezing device (Vitrobot, FEI. 12°C, 8-12s blot time, blot force 8, humidity 100%).

Grids of KR4000 and KR4103 were imaged on a Jeol3100 cryoTEM operating at 300kV with in column omega energy filter and K2 direct electron camera. Grids of KR4102 and KR3906 were imaged on a Krios Cryo TEM (FEI) operating at 300kV with post column energy filter (Quantum, GATAN) and K2 direct electron camera. All data were collected with the automatic data collection program serialEM (Mastonarde, 2005). Square overview images were acquired using a defocus of 80-100 microns at a nominal magnification of 3600-6500x (Krios) or 1200x (Jeol) using the polygon montage operation (specimen pixel size: 33-67Å). Beam intensity was set to 8e⁻/px/s over an empty hole and exposure times ranged from 2-5s depending on ice thickness. Bidirectional tomographic tilt series were collected from ±60° using a defocus of 6-8 µm and at a magnification which provided specimen pixel size of 4-7 Å. Total dose of the tilt series were kept between 60-90 e⁻/Å². All tilt series images were collected in movie mode and the frames aligned using MotionCor2 (Zheng et al., 2017), Aligned frames were compiled into stacks and processed using IMOD (Kremer et al., 1996). Contrast of resulting tomograms was enhanced using a non-linear anisotropic diffusion filter (Frangakis and Hegerl, 2001) and manually segmented using the 3D visualization program AMIRA (ThermoFisher).

RB-Tnseq analysis. A 1 ml aliquot of the RB-Tnseq library in NA1000 (Price et al., 2018) was thawed and grown to $OD_{660} = 0.65$ in 25 ml PYE medium with kanamycin. Aliquots of this culture were saved for sequencing of pre-challenge barcodes, or were diluted to $OD_{660} = 0.02$ in PYE medium (set8IT011, set8IT023, and set8IT035) or PYE medium with 2 µg/ml CHIR-090 (set8IT012, set8IT024, and set8IT036). Cultures were grown for 9 hours at 30°C as described (Price et al., 2018) before cells were harvested and post-challenge barcodes were sequenced. Gene fitness (f) and significance (t) scores were calculated as described (Wetmore et al., 2015). Candidate genes examined in this study ($CCNA_01217-01220$) had fitness scores between -1.5 and -3.7, with signficance scores between -3.0 and -8.4, for individual trials of library growth in PYE + CHIR-090.

Extraction and liquid chromatography-tandem mass spectrometry (LC-MS/MS) of sphingolipids. *Caulobacter* strains were grown overnight with or without 0.5 mM vanillate (5 ml), and lipids were extracted by the method of Bligh and Dyer (Bligh and Dyer, 1959). Cells were harvested and resuspended in 1 ml of water, 3.75 ml of 1:2 (v/v) chloroform: methanol was added, and the samples were mixed by vortexing. Chloroform (1.25 ml) and water (1.25 ml) were added sequentially with vortexing to create a two-phase system and the samples were

centrifuged at 200 x g for 5 minutes at room temperature. The bottom, organic phase was transferred to a clean glass tube with a Pasteur pipette and washed twice in "authentic" upper phase. Subsequently, the organic phase containing lipids was collected and dried under argon. Our methods for lipid analysis by normal phase LC/ESI–MS/MS have been described (Guan et al., 2014). Briefly, normal phase LC was performed on an Agilent 1200 Quaternary LC system equipped with an Ascentis Silica HPLC column, 5 μ m, 25 cm × 2.1 mm (Sigma-Aldrich, St. Louis, MO) as described. The LC eluent (with a total flow rate of 300 μ l/min) was introduced into the ESI source of a high resolution TripleTOF5600 mass spectrometer (Applied Biosystems, Foster City, CA). Instrumental settings for negative ion ESI and MS/MS analysis of lipid species were as follows: ion spray voltage (IS) = -4500 V; curtain gas (CUR) = 20 psi; ion source gas 1 (GSI) = 20 psi; declustering potential (DP) = -55 V; and focusing potential (FP) = -150 V. The MS/MS analysis used nitrogen as the collision gas. Data analysis was performed using Analyst TF1.5 software (Applied Biosystems, Foster City, CA).

Data Availability Statement

Sequence data that support the findings of this study are openly available in the Sequence Read Archive at https://www.ncbi.nlm.nih.gov/sra, under BioProject ID PRJNA526705, with specific NCBI BioSample accession numbers listed in **Table S3**. RB-Tnseq data are accessible at https://fit.genomics.lbl.gov/, with set and index numbers listed under RB-Tnseq analysis.

Supplemental Information Titles and Legends

Figure S1, related to Fig. 1: Morphology, growth, and complementation of strains in which suppressor mutations permit the loss of ctpA. (A) Isolates from the $\Delta ctpA$ suppressor screen show variations in morphology. DIC images of selected suppressor isolates confirmed to have lost the ctpA covering plasmid. Putative suppressor mutations identified by whole-genome resequencing are indicated. Scale bar, 3 μ m. (B) Growth curves of the indicated strains in PYE

1070 showing (i or iii) OD_{660} and (ii or iv) colony-forming units (CFU) per mL (mean \pm S.D., N=3). (C) 1071 Viability assays of $\triangle ctpA$ suppressor mutants, each harboring a vector for xylose-driven 1072 expression of the corresponding suppressor gene or the cerulean gene as a control. Kanamycin 1073 was included in media to retain expression vectors. 1074 1075 Figure S2, related to Fig.1: A subset of ctpA suppressor mutations impair or block S-LPS 1076 production. (A) q-S-LPS-probed immunoblot and (B) Pro-Q Emerald 300-stained gel of 1077 Proteinase K-treated whole-cell lysates of the indicated strains. (C) Complementation of O-1078 antigen biosynthesis using plasmid-borne genes driven by a xylose-inducible promoter. Pro-Q 1079 Emerald 300-stained polyacrylamide gel of Proteinase K-treated whole-cell lysates of the 1080 indicated strains grown in either PYED (D) or PYEX (X). Samples were normalized by OD₆₆₀. *** 1081 = S-LPS. ** = putative full-length lipid A-core polysaccharide. * = putative incomplete lipid A-1082 core species in cells lacking manC activity (CCNA 03733). 1083 1084 Figure S3, related to Figure 2: $\triangle ctpA$ and $\triangle lpxC$ strains with suppressor mutations lack wild-1085 type lipid A. Tandem mass spectrometry (MSMS)-derived structures of lipid A from the indicated 1086 strains. Lipid extraction and MSMS analysis were performed using the same protocols for all 1087 strains. 1088 1089 Movie S1, related to Figure 2. Tomogram of Caulobacter crescentus NA1000 grown to mid-1090 exponential phase in PYE. 1091 1092 **Movie S2, related to Figure 2.** Tomogram of $\Delta ctpA$ $\Delta sspB$ Δfur grown to mid-exponential 1093 phase in PYE. 1094 1095 **Movie S3, related to Figure 2.** Tomogram of $\Delta lpxC \Delta sspB \Delta fur$ grown to mid-exponential 1096 phase in PYE. 1097 1098 **Movie S4, related to Figure 2.** Tomogram of $\triangle ctpA$ $\triangle sspB$ + pJS14-P_{xy/x}-ctpA-3xFLAG-ssrA 1099 grown to mid-exponential phase in PYEX, washed twice with PYE, released into PYED at OD₆₆₀ 1100 = 0.02, and incubated for 10 hours before harvest. 1101 1102 Figure S4, related to Figure 6: The total ion chromatogram of the C. crescentus lipidome 1103 shows the major lipid species present. DAG: diacylglycerol; MHDAG: mono-hexosyl

- 1104 diacylglycerol; FA: fatty acids; PG: phosphatidylglycerol; HexA-DAG: hexuronic acid-
- diacylglycerol; CPG: ceramide phosphoglycerate.
- 1107 Figure S5, related to Figure 3. Slow growth at a reduced temperature in rich medium is
- insufficient for viability of $\Delta lpxC$ strains. (A) Viability of the LpxC depletion strain grown in
- inducing (PYEX) or depleting (PYED) conditions, at the indicated temperatures. (B) Viability of
- 1110 the stable $\Delta lpxC \Delta fur \Delta sspB$ strain harboring a Pxyl-fur plasmid, grown in noninducing (PYED)
- or inducing (PYED) conditions, at the indicated temperatures. Cells were plated from 10-fold
- serially diluted suspensions normalized to $OD_{660} = 0.1$. Plates were incubated for 3 days (30°C)
- or 6 days (22°C) and are representative of at least three independent trials. Plates in B included
- 1114 kanamycin to retain the *fur* expression vector.
- 1116 **Table S1, related to Figure 1:** Single-nucleotide polymorphisms and indels in $\Delta ctpA$
- 1117 suppressors.

1115

1118

1121

1123

1125

1127

1129

- 1119 **Table S2**, **related to Figure 3**: Single-nucleotide polymorphisms and indels in $\Delta lpxC$
- 1120 suppressors.
- **Table S3, related to Figure 3:** Growth rates in PYE medium at 22°C.
- 1124 Table S4, related to STAR Methods: Strains used in this study.
- 1126 **Table S5**, **related to STAR Methods**: Plasmids used in this study.
- 1128 Table S6, related to STAR Methods: Primers used in this study.
- 1130 References
- 1131 Afgan, E., Baker, D., Beek, M. van den, Blankenberg, D., Bouvier, D., Cech, M., Chilton, J.,
- 1132 Clements, D., Coraor, N., Eberhard, C., et al. (2016). The Galaxy platform for accessible,
- 1133 reproducible and collaborative biomedical analyses: 2016 update. Nucleic Acids Res. 44, W3-
- 1134 W10.
- 1136 Andrews, S., Norton, I., Salunkhe, A.S., Goodluck, H., Aly, W.S.M., Mourad-Agha, H., and
- 1137 Cornelis, P. (2013). Control of iron metabolism in bacteria. Met. lons Life Sci. 12, 203–239.

- Awram, P., and Smit, J. (2001). Identification of lipopolysaccharide O antigen synthesis genes
- required for attachment of the S-layer of Caulobacter crescentus. Microbiology 147, 1451–1460.
- 1142 Bligh, E.G., and Dyer, W.J. (1959). A rapid method of total lipid extraction and purification. Can
- 1143 J. Biochem. Physiol. 37, 911–917.

1141

1144

1148

1152

1158

1162

1166

- Blondelet-Rouault, M.H., Weiser, J., Lebrihi, A., Branny, P., and Pernodet, J.L. (1997). Antibiotic
- resistance gene cassettes derived from the omega interposon for use in E. coli and
- 1147 Streptomyces. Gene 190, 315–317.
- Boll, J.M., Crofts, A.A., Peters, K., Cattior, V., Vollmer, W., Davies, B.W., and Trent, M.S.
- 1150 (2016). A penicillin-binding protein inhibits selection of colistin-resistant, lipooligosaccharide-
- deficient Acinetobacter baumannii. Proc. Natl. Acad. Sci. USA 113, E6228–E6237.
- Brown, D.B., Forsberg, L.S., Kannenberg, E.L., and Carlson, R.W. (2012). Characterization of
- galacturonosyl transferase genes rgtA, rgtB, rgtC, rgtD, and rgtE responsible for
- 1155 lipopolysaccharide synthesis in nitrogen-fixing endosymbiont Rhizobium leguminosarum:
- 1156 lipopolysaccharide core and lipid galacturonosyl residues confer membrane stability. J. Biol.
- 1157 Chem. 287, 935–949.
- Brown, D.B., Muszynski, A., and Carlson, R.W. (2013). Elucidation of a novel lipid A alpha-(1,1)-
- 1160 GalA transferase gene (rgtF) from Mesorhizobium loti: Heterologous expression of rgtF causes
- 1161 Rhizobium etli to synthesize lipid A with alpha-(1,1)-GalA. Glycobiology 23, 546–558.
- 1163 Christen, B., Abeliuk, E., Collier, J.M., Kalogeraki, V.S., Passarelli, B., Coller, J.A., Fero, M.J.,
- 1164 McAdams, H.H., and Shapiro, L. (2011). The essential genome of a bacterium. Mol. Syst. Biol.
- **1165** *7*, 528.
- 1167 Crosson, S., McGrath, P.T., Stephens, C., McAdams, H.H., and Shapiro, L. (2005). Conserved
- modular design of an oxygen sensory/signaling network with species-specific output. Proc. Natl.
- 1169 Acad. Sci. USA 102, 8018–8023.
- 1171 Darveau, R.P., and Hancock, R.E. (1983). Procedure for isolation of bacterial
- 1172 lipopolysaccharides from both smooth and rough Pseudomonas aeruginosa and Salmonella
- 1173 typhimurium strains. J. Bacteriol. 155, 831–838.

- Davis, M.R.J., and Goldberg, J.B. (2012). Purification and visualization of lipopolysaccharide
- from Gram-negative bacteria by hot aqueous-phenol extraction. J. Vis. Exp. e3916.
- 1178 De Castro, C., Molinaro, A., Lanzetta, R., Silipo, A., and Parrilli, M. (2008). Lipopolysaccharide
- 1179 structures from Agrobacterium and Rhizobiaceae species. Carbohydr. Res. 343, 1924–1933.
- 1180 Dehio, C., and Meyer, M. (1997). Maintenance of broad-host-range incompatibility group P and
- 1181 group Q plasmids and transposition of Tn5 in Bartonella henselae following conjugal plasmid
- transfer from Escherichia coli. J. Bacteriol. 179, 538–540.
- 1184 El Hamidi, A., Tirsoaga, A., Novikov, A., Hussein, A., and Caroff, M. (2005). Microextraction of
- 1185 bacterial lipid A: Easy and rapid method for mass spectrometric characterization. J. Lipid Res.
- 1186 *46*, 1773–1778.

1177

1183

1187

1191

1195

1198

1201

1205

- Ely, B. (1991). Genetics of Caulobacter crescentus. Methods Enzymol. 204, 372–384.
- 1189 Evinger, M., and Agabian, N. (1977). Envelope-associated nucleoid from Caulobacter
- 1190 crescentus stalked and swarmer cells. J. Bacteriol. 132. 294–301.
- 1192 Fontenot, C.R., Tasnim, H., Valdes, K.A., Popescu, C.V., and Ding, H. (2020). Ferric uptake
- 1193 regulator (Fur) reversibly binds a [2Fe-2S] cluster to sense intracellular iron homeostasis in
- 1194 Escherichia coli. J. Biol. Chem. 295, 15454–15463.
- 1196 Frangakis, A.S., and Hegerl, R. (2001). Noise reduction in electron tomographic reconstructions
- using nonlinear anisotropic diffusion. J. Struct. Biol. 135, 239–250.
- 1199 Gilchrist, A., and Smit, J. (1991). Transformation of freshwater and marine caulobacters by
- 1200 electroporation. J. Bacteriol. *173*, 921–925.
- 1202 Guan, Z., Katzianer, D., Zhu, J., and Goldfine, H. (2014). Clostridium difficile contains
- 1203 plasmalogen species of phospholipids and glycolipids. Biochim. Biophys. Acta 1842, 1353–
- 1204 1359.
- 1206 Hassett, D.J., Britigan, B.E., Svendsen, T., Rosen, G.M., and Cohen, M.S. (1987). Bacteria form
- 1207 intracellular free radicals in response to paraguat and streptonigrin. Demonstration of the
- 1208 potency of hydroxyl radical. J. Biol. Chem. 262, 13404–13408.

- Henry, R., Crane, B., Powell, D., Lucas, D.D., Li, Z., Aranda, J., Harrison, P., Nation, R.L.,
- 1211 Adler, B., Harper, M., et al. (2015). The transcriptomic response of Acinetobacter baumannii to
- 1212 colistin and diripenem alone and in combination in an in vitro
- pharmacokinetics/pharmacodynamics model. J. Antimicrob. Chermother. 70, 1303–1313.
- Hershey, D.M., Fiebig, A., and Crosson, S. (2019). A genome-wide analysis of adhesion in
- 1216 Caulobacter crescentus identifies new regulatory and biosynthetic components for holdfast
- 1217 assembly. mBio 10, 2273.
- Jones, M.D., Vinogradov, E., Nomellini, J.F., and Smit, J. (2015). The core and O-
- 1220 polysaccharide structure of the Caulobacter crescentus lipopolysaccharide. Carbohydr. Res.
- 1221 *402*, 111–117.

1218

1222

1226

1230

1234

1238

- Justino, M.C., Almeida, C.C., Teixeira, M., and Saraiva, L.M. (2007). Escherichia coli di-iron
- YtfE protein is necessary for the repair of stress-damaged iron-sulfur clusters. J. Biol. Chem.
- 1225 282, 10352–10359.
- 1227 Karbarz, M.J., Kalb, S.R., Cotter, R.J., and Raetz, C.R.H. (2003). Expression cloning and
- 1228 biochemical characterization of a Rhizobium leguminosarum lipid A 1-phosphatase. J. Biol.
- 1229 Chem 278, 39269–39279.
- 1231 Kawahara, K., Seydel, U., Matsuura, M., Danbara, H., Rietschel, E.T., and Zahringer, U. (1991).
- 1232 Chemical structure of glycosphingolipids isolated from Sphingomonas paucimobilis. FEBS Lett.
- 1233 292, 107–110.
- 1235 Kawasaki, S., Moriguchi, R., Sekiya, K., Nakai, T., Ono, E., Kume, K., and Kawahara, K. (1994).
- 1236 The cell envelope structure of the lipopolysaccharide-lacking Gram-negative bacterium
- 1237 Sphingomonas paucimobilis. J. Bacteriol. 176, 284–290.
- 1239 Kremer, J.R., Mastonarde, D.N., and McIntosh, J.R. (1996). Computer visualization of three-
- dimensional image data using IMOD. J. Struct. Biol. *116*, 71–76.
- 1242 Leaden, L., Silva, L.G., Ribiero, R.A., Santos, N.M.D., Lorenzetti, A.P.R., Alegria, T.G.P.,
- 1243 Schultz, M.L., Medeiros, M.H.G., Koide, T., and Marques, M.V. (2018). Iron deficiency
- 1244 generates oxidative stress and activation of the SOS response in Caulobacter crescentus.
- 1245 Front. Microbiol. 9, 2014.

- Leung, L.M., Fondrie, W.E., Doi, Y., Johnson, J.K., Strickland, D.K., Ernst, R.K., and Goodlett,
- 1248 D.R. (2017). Identification of the ESKAPE pathogens by mass spectrometric analysis of
- microbial membrane glycolypids. Sci. Rep. 7, 6403.
- 1250 Levchenko, I., Seidel, M., Sauer, R.T., and Baker, T.A. (2000). A specificity-enhancing factor for
- the ClpXP degradation machine. Science 289, 2354–2356.
- Liu, L., Feng, X., Wang, W., Chen, Y., Chen, Z., and Gao, H. (2020). Free Rather Than Total
- 1254 Iron Content Is Critically Linked to the Fur Physiology in Shewanella oneidensis. Front.
- 1255 Microbiol. 11, 593246.

1252

1256

1261

1265

1268

1272

1275

- 1257 Mamat, U., Meredith, T.C., Aggarwal, P., Kuhl, A., Kirchoff, P., Lindner, B., Hanuszkiewicz, A.,
- 1258 Sun, J., Holst, O., and Woodard, R.W. (2008). Single amino acid substitutions in either YhjD or
- 1259 MsbA confer viability to 3-deoxy-D-manno-oct-2-ulosonic acid-depleted Escherichia coli. Mol.
- 1260 Microbiol. 67, 633–648.
- Marks, M.E., Castro-Rojas, C., Teiling, C., Du, L., Kapatral, V., Walunas, T.L., and Crosson, S.
- 1263 (2010). The genetic basis of laboratory adaptation in Caulobacter crescentus. J. Bacteriol. 192,
- 1264 3678–3688.
- 1266 Mastonarde, D.N. (2005). Automated electron microscope tomography using robust prediction
- of specimen movements. J. Struct. Biol. 152, 36–51.
- 1269 McClerren, A.L., Endsley, S., Bowman, J.L., Andersen, N.H., Guan, Z., Rudolph, J., and Raetz,
- 1270 C.R. (2005). A slow, tight-binding inhibitor of the zinc-dependent deacetylase LpxC of lipid A
- biosynthesis with antibiotic activity comparable to ciprofloxacin. Biochemistry 44, 16574–16583.
- 1273 Meisenzahl, A.C., Shapiro, L., and Jenal, U. (1997). Isolation and characterization of a xylose-
- dependent promoter from Caulobacter crescentus. J. Bacteriol. 179, 592–600.
- 1276 Meredith, T.C., Aggarwal, P., Mamat, U., Lindner, B., and Woodard, R.W. (2006). Redefining
- the requisite lipopolysaccharide structure in Escherichia coli. ACS Chem. Biol. 1, 33–42.
- 1279 Moffatt, J.H., Harper, M., Harrison, P., Hale, J.D., Vinogradov, E., Seemann, T., Henry, R.,
- 1280 Crane, B., Michael, F.S., Cox, A.D., et al. (2010). Colistin resistance in Acinetobacter baumannii

- is mediated by complete loss of lipopolysaccharide production. Antimicrob. Agents Chemother.
- 1282 *54*, 4971–4977.

1289

1293

1296

1299

1304

1308

- Moffatt, J.H., Harper, M., and Boyce, J.D. (2019). Mechanisms of polymyxin resistance. Adv.
- 1285 Exp. Med. Biol. 55-71.
- 1286 Nachin, L., El Hassouni, M., Loiseau, L., Expert, D., and Barras, F. (2001). SoxR-dependent
- response to oxidative stress and virulence of Erwinia chrysanthemi: the key role of SufC, an
- 1288 orphan ABC ATPase. Mol. Microbiol. 39, 960–972.
- 1290 Nagiec, M.M., Skrzypek, M., Nagiec, E.E., Lester, R.L., and Dickson, R.C. (1998). The LCB4
- 1291 (YOR171c) and LCB5 (YLR260w) genes of Saccharomyces encode sphingoid long chain base
- 1292 kinases. J. Biol. Chem. 273, 19437–19442.
- 1294 Nagy, E., Losick, R., and Kahne, D. (2019). Robust suppression of lipopolysaccharide
- deficiency in Acinetobacter baumannii by growth in minimal medium. J. Bacteriol. 201, 420.
- 1297 Nikaido, H. (2003). Molecular basis of bacterial outer membrane permeability revisited.
- 1298 Microbiol. Mol. Biol. Rev. 67, 593–656.
- 1300 Olea-Ozuna, R.J., Poggio, S., Bergström, E., Quiroz-Rocha, E., García-Soriano, D.A.,
- 1301 Sahonero-Canavesi, D.X., Padilla-Gómez, J., Martínez-Aguilar, L., López-Lara, I.M., Thomas-
- Oates, J., et al. (2021). Five structural genes required for ceramide synthesis in Caulobacter
- and for bacterial survival. Environ. Microbiol. 23, 143–159.
- 1305 Peng, D., Hong, W., Choudhury, B.P., Carlson, R.W., and Gu, X.-X. (2005). Moraxella
- 1306 cararrhalis bacterium without endotoxin, a potential vaccine candidate. Infect. Immun. 73, 7569–
- 1307 7577.
- 1309 Plötz, B.M., Lindner, B., Stetter, K.O., and Holst, O. (2000). Characterization of a novel lipid A
- 1310 containing D-galacturonic acid that replaces phosphate residues. The structure of the lipid a of
- the lipopolysaccharide from the hyperthermophilic bacterium Aquifex pyrophilus. J. Biol. Chem.
- 1312 275, 11222–11228.
- 1314 Price, M.N., Wetmore, K.M., Waters, R.J., Callaghan, M., Ray, J., Liu, H., Kuehl, J.V., Melnyk,
- 1315 R.A., Lamson, J.S., Suh, Y., et al. (2018). Mutant phenotypes for thousands of bacterial genes
- 1316 of unknown function. Nature *557*, 503–509.

- 1318 Qureshi, N., Takayama, K., Mascagni, P., Honovich, J., Wong, R., and Cotter, R.J. (1988).
- 1319 Complete structural determination of lipopolysaccharide obtained from deep rough mutant of
- 1320 Escherichia coli. Purification by high performance liquid chromatography and direct analysis by
- plasma desorption mass spectrometry. J. Biol. Chem. 263, 11971–11976.
- 1323 Radolf, J.D., and Kumar, S. (2018). The Treponema pallidum outer membrane. Curr. Top.
- 1324 Microbiol. Immuno. 415, 1–38.
- Rojas, E.R., Billings, G., Odermatt, P.D., Auer, g K., Zhu, L., Miguel, A., Chang, F., Weibel,
- 1327 D.B., Theriot, J.A., and Huang, K.C. (2018). The outer membrane is an essential load-bearing
- element in Gram-negative bacteria. Nature 559, 617–621.
- 1330 Samuel, G., and Reeves, P. (2003). Biosynthesis of O-antigens: Genes and pathways involved
- in nucleotide sugar precursor synthesis and O-antigen assembly. Carboyhdr. Res. 338, 2503–
- 1332 2519.

1322

1325

1329

1333

1337

1341

1344

1348

- 1334 Shapland, E.B., Reisinger, S.J., Bajwa, A.K., and Ryan, K. (2011). An essential tyrosine
- phosphatase homolog regulates cell separation, outer membrane integrity, and morphology in
- 1336 Caulobacter crescentus. J. Bacteriol. 193, 4361–4370.
- da Silva Neto, J.F., Braz, V.S., Italiani, V.C.S., and Margues, M.V. (2009). Fur controls iron
- 1339 homeostasis and oxidative stress defense in the oligotrophic alpha-proteobacterium
- 1340 Caulobacter crescentus. Nucleic Acids Res. 37, 4812–4825.
- da Silva Neto, J.F., Lourenco, R.F., and Marques, M.V. (2013). Global transcriptional response
- of Caulobacter crescentus to iron availability. BMC Genomics 14, 549.
- 1345 Simpson, B.W., Nieckarz, M., Pinedo, V., McLean, A.B., Cava, F., and Trent, M.S. (2021).
- 1346 Acinetobacter baumannii Can Survive with an Outer Membrane Lacking Lipooligosaccharide
- Due to Structural Support from Elongasome Peptidoglycan Synthesis. mBio *12*, e0309921.
- 1349 Skerker, J.M., Prasol, M.S., Perchuk, B.S., Biondi, E.G., and Laub, M.T. (2005). Two-
- 1350 component signal transduction pathways regulating growth and cell cycle progresion in a
- 1351 bacterium: A systems-level analysis. PLoS Biol. 3, e334.

- Smit, J., Kaltashov, I.A., Cotter, R.J., Vinogradov, E., Perry, M.B., Haider, H., and Qureshi, N.
- 1354 (2008). Structure of a novel lipid A obtained from the lipopolysaccharide of Caulobacter
- 1355 crescentus. Innate Immun. *14*, 25–37.
- 1357 Stankeviciute, G., Guan, Z., Goldfine, H., and Klein, E.A. (2019). Caulobacter crescentus adapts
- 1358 to phosphate starvation by synthesizing anionic glycoglycerolipids and a novel
- 1359 glycosphingolipid. mBio *10*, 107.
- 1361 Stankeviciute, G., Tang, P., Ashley, B., Chamberlain, J.D., Hansen, M.E.B., Coleman, A.,
- 1362 D'Emilia, R., Fu, L., Mohan, E.C., Nguyen, H., et al. (2021). Convergent evolution of bacterial
- 1363 ceramide synthesis. Nat. Chem. Biol. DOI: 10.1038/s41589-021-00948-7.
- 1365 Steeghs, L., Hartog, R. den, Boer, A. den, Zomer, B., Roholl, P., and Ley, P. van der (1998).
- 1366 Meningitis bacterium is viable without endotoxin. Nature 392, 449–450.
- 1368 Thanbichler, M., Iniesta, A.A., and Shapiro, L. (2007). A comprehensive set of plasmids for
- vanillate- and xylose-inducible gene expression in Caulobacter crescentus. Nucleic Acids Res.
- 1370 35, e137.

1360

1364

1367

1371

1375

1378

1382

- 1372 Toh, E., Jr, H.D.K., and Brun, Y.V. (2008). Characterization of the Caulobacter crescentus
- 1373 holdfast polysaccharide biosynthesis pathway reveals significant redundancy in the initiating
- 1374 glycosyltransferase and polyerase steps. J. Bacteriol. 190, 7219–7131.
- 1376 Velkov, T., Thompson, P.E., Nation, R.L., and Li, J. (2010). Structure--activity relationships of
- polymyxin antibiotics. J. Med. Chem. 53, 1898–1916.
- 1379 Walker, S.G., Karunaratne, D.N., Ravenscroft, N., and Smit, J. (1994). Characterization of
- 1380 mutants of Caulobacter crescentus defective in surface attachment of the paracrystalline
- 1381 surface layer. J. Bacteriol. 176, 6313–6323.
- 1383 Wang, X., Ribeiro, A.A., Guan, Z., McGrath, S.C., Cotter, R.J., and Raetz, C.R.H. (2006).
- 1384 Structure and biosynthesis of free lipid A molecules that replace lipopolysaccharide in
- 1385 Francisella tularensis subsp. novicida. Biochemistry 45, 14427–14440.
- 1387 Westphal, O., and Jann, K. (1965). Bacterial lipopolysaccharides extraction with phenol-water
- and further applications of the procedure. Methods Carbohydr. Chem. 5, 83–91.

- 1390 Wetmore, K.M., Price, M.N., Waters, R.J., Lamson, J.S., He, J., Hoover, C.A., Blow, M.J.,
- Bristow, J., Butland, G., Arkin, A.P., et al. (2015). Rapid quantification of mutant fitness in
- diverse bacteria by sequencing randomly bar-coded transposons. mBio *6*, e00306–e00315.
- Whitfield, C., and Trent, M.S. (2014). Biosynthesis and export of bacterial lipopolysaccharides.
- 1395 Annu. Rev. Biochem. 83, 99–128.

1393

1396

1400

1403

1408

1411

1415

- Wofford, J.D., Bolaji, N., Dziuba, N., Outten, F.W., and Lindahl, P.A. (2019). Evidence that a
- respiratory shield in Escherichia coli protects a low-molecular-mass Fell pool from O2-
- dependent oxidation. J. Biol. Chem. 294, 50–62.
- 1401 Yeowell, H.N., and White, J.R. (1982). Iron requirement in the bactericidal mechanism of
- streptonigrin. Antimicrob. Agents Chemother. 22, 961–968.
- 1404 Yoon, S.H., Liang, T., Schneider, T., Oyler, B.L., Chandler, C.E., Ernst, R.K., Yen, G.S., Huang,
- 1405 Y., Nilsson, E., and Goodlett, D.R. (2016). Rapid lipid a structure determination via surface
- 1406 acoustic wave nebulization and hierarchical tandem mass spectrometry algorithm. Rapid
- 1407 Commun. Mass Spectrom. 30, 2555–2560.
- 1409 Zhang, G., Meredith, T.C., and Kahne, D. (2013). On the essentiality of lipopolysaccharide to
- 1410 Gram-negative bacteria. Curr. Opin. Microbiol. 16, 779–785.
- 1412 Zheng, S.Q., Plaovcak, E., Armache, J.P., Verba, K.A., Cheng, Y., and Agard, D.A. (2017).
- 1413 MotionCor2: anisotropic correction of bean-induced motion for improved cryo-electron
- 1414 microscopy. Nat. Methods *14*, 331–332.
- 1416 Zhou, B., Schrader, J.M., Kalogeraki, V.S., Abeliuk, E., Dinh, C.B., Pham, J.Q., Cui, Z.Z., Dill,
- 1417 D.L., McAdams, H.H., and Shapiro, L. (2015). The global regulatory architecture of transcription
- during the Caulobacter cell cycle. PLoS Genet. 11, e1004831.

Supplementary Tables

Table S1, related to Figure 1: Single-nucleotide polymorphisms and indels in $\Delta ctpA$

suppressors^a

14241425

1421

Strain	Sequence	Gene ^c	Annotation	Base	Amino Acid
	position ^b			Change	Substitution
S3	1668695	01553	Undecaprenyl-phosphate beta-N-acetyl-D-	G>T	K54N
			fucosaminephosphotrans-		
			ferase		
	2383967	02235	SGNH hydrolase family protein	G>A	G109D
S8	3492550	03316	UDP-N-acetylglucosamine 4,6-	AG>ATG	E487Frameshift
			dehydratase/UDP-D-quinovosamine 4-		
			dehydrogenase		
S16	58496	00055	Ferric uptake regulation protein	A>T	L38Q
S21	515085	00497	Putative rhamnosyl transferase	G>A	G263D
	1378399	01250	FecCD-family transporter protein	GCC>GC	A340Frameshift
S32	1157376	01056	Methyltransferase	A>AG	S31Framshift
	2164248	02016	nuoMNADH-quinone oxidoreductase chain M	C>T	M7I
	2949436	02792	TonB-dependent outer membrane receptor	A>G	S516G
S36	3901011	03733	Mannose-1-phosphate guanylyltransferase	C>T	W279Stop
S38	726779	00669	Glycosyltransferase family 99 protein WbsX	CTG>CG	Q476Frameshift
S40	378822	00362	Zinc uptake regulation protein	A>T	C156S
	2868272	-	-	G>C	-
	3913883	03744	dTDP-glucose 4,6-dehydratase	T>A	I269F
S43	1377138	01249	ABC-transporter substrate binding protein	C>T	A169V
	1668861	01553	Undecaprenyl-phosphate beta-N-acetyl-D-	CC>GA	P110E
			fucosaminephosphotransferase		
	2976030	02820	TadG-family protein	C>T	Silent
S44	727833	00669	Glycosyltransferase family 99 protein WbsX	A>C	L125R
S47	537654	00524	Conserved hypothetical cytosolic protein	A>AG	L369Frameshift
	1173251	01068	Glycosyltransferase	GCC>GC	R293Frameshift
S52	514656	00497	Putative rhamnosyl transferase	T>G	L120R
	810384	00752	3-hydroxybutyryl-CoA dehydrogenase	T>A	Stop>Y
	3797776	-	-	T>C	-
S53	58379	00055	Ferric uptake regulation protein	G>T	S77Stop

	1778110	01656	Endonuclease/exonuclease/phosphatase	A>C	L4R
			family protein		
	3900664	03733	Mannose-1-phosphate guanylyltransferase	G>A	Q395Stop
S54	1377127	01249	ABC-transporter substrate binding protein	CGG>CG	G166Frameshif
	3492771	03316	UDP-N-acetylglucosamine 4,6-	G>A	E561K
			dehydratase/UDP-D-quinovosamine 4-		
			dehydrogenase		
S57	1492703	01378	Protein-L-isoaspartate O-methyltransferase	G>GC	G59Frameshift
	2487074	02347	Phosphomannomutase/phosphoglucomutase	G>A	G266D
S111	295119	00283	2,3,4,5-tetrahydropyridine-2,6-dicarboxylate	A>T	L284Q
			N-succinyltransferase		
	1173965	01068	Glycosyltransferase	TGC>T	R55Frameshift
S112	311705	00297	Two-component response regulator	C>T	W64Stop
	315570	00301	Phosphotransferase family protein	T>G	I319S
	2487307	02347	Phosphomannomutase/phosphoglucomutase	G>A	E344K
	3569520	03399	Flavin prenyltransferase UbiX	C>T	A159T

1427 aln addition to the indicated mutations, each strain is also $\Delta ctpA \Delta sspB$.

1428 ^bSequence positions refer to the genome of *Caulobacter crescentus* NA1000 (NC_011916.1).

°The prefix for each gene number is CCNA_.

Table S2, related to Figure 3: Single-nucleotide polymorphisms and indels identified in $\Delta lpxC$ suppressors^a

Strain	Sequence	Gene ^c	Annotation	Base	Amino Acid
	position ^b			Change	Substitution
S1	58446	00055	Ferric uptake regulation protein Fur	A>T	Y55N
	4000704	03835	3-oxoacyl-(Acyl-carrier-protein) synthase	C>T	G396S
S5	58436	00055	Ferric uptake regulation protein Fur	A>T	V58E

^aIn addition to the indicated mutations, each strain is also $\Delta lpxC \Delta sspB \Delta 00497$.

^bSequence positions refer to the genome of *Caulobacter crescentus* NA1000 (NC_011916.1).

^{1438 °}The prefix for each gene number is *CCNA*_.

Table S3, related to Figure 3: Growth rates in PYE medium at 22°C.

Doubling time +/- standard		
deviation (hours) ^a		
Strain	PYE 30°C	PYE 22°C
NA1000	1.61 +/- 0.04	2.50 +/- 0.17
ΔsspB	1.51 +/- 0.04	2.44 +/- 0.09
∆fur ∆sspB	1.77 +/- 0.08	3.16 +/- 0.21

^aDoubling times were calculated from optical density measurements (660 nm) during exponential growth.

Table S4, related to STAR Methods: Strains used in this study.

Strain	Description	Note	NCBI BioSample	Reference
Number			Accessions	
KR4000	Wild-type Caulobacter NA1000			(Evinger and
				Agabian,
KR3180	NA1000 pJS14			1977) This study
KKS100	NA 1000 p33 14			This study
KR1499	ΔsspB::aadA			(Shapland et
	,			al., 2011)
KR3877	ΔCCNA_00497::hyg			This study
KR4198	ΔCCNA_00497::hyg pJS14			This study
KR3871	ΔCCNA_01553::hyg			This study
KK307 I				This study
KR4197	ΔCCNA_01553::hyg pJS14			This study
	_ ,,,,,,,,,,,,,,,,,,,,,,,,,,,,,,,,,,,,,			
KR4076	Δfur::hyg			This study
1/0.4400	A.C. (1044			T1: 1
KR4199	Δ <i>fur::hyg</i> pJS14			This study
KR3953	ΔCCNA_00497::hyg ΔsspB::aadA			This study
11110000				Tillo otday
KR4115	ΔCCNA_01055::hyg ΔsspB::aadA			This study
KR4116	ΔCCNA_01068::hyg ΔsspB::aadA			This study
KR3954	ΔCCNA_01553::hyg ΔsspB::aadA			This study
KK3934	ΔCCNA_01333IIyg ΔSSpbaadA			This study
KR3955	ΔCCNA 03733::hyg ΔsspB::aadA			This study
	_ ,,,			
KR4077	Δfur::hyg ΔsspB::aadA			This study
1/5 / / 50				
KR4153	ΔsspB::aadA pXCERN-2			This study
KR4154	ΔCCNA 00497::hyg ΔsspB::aadA			This study
1414104	pXCERN-2			Tino Study
KR4155	ΔCCNA 01553::hyg ΔsspB::aadA			This study
	pXCERN-2			
KR4156	ΔCCNA_03733::hyg ΔsspB::aadA			This study
	pXCERN-2			
KR4157	Δfur::hyg ΔsspB::aadA pXCERN-2			This study
VD4450	A CCN/A 00407::b::			This start
KR4158	ΔCCNA_00497::hyg ΔsspB::aadA pZlK172			This study
KR4159	ΔCCNA 01553::hyg ΔsspB::aadA			This study
1114108	pZIK173			Tills Study
	P=11110			

KR4160	ΔCCNA_03733::hyg ΔsspB::aadA pZIK174			This study
KR4161	Δfur::hyg ΔsspB::aadA pZIK175			This study
KR4269	Δfur::hyg ΔsspB::aadA pZIK197			This study
KR3906	ΔctpA::tetAR ΔsspB::aadA pAB6	Restock of KR2423		(Shapland et
LCD 4444	A (A ((A D A)	from Shapland 2011	0.4.4.4.0.5.0.7.0.0	al., 2011)
KR4111	ΔctpA::tetAR ΔsspB::aadA ΔCCNA_00497::hyg pAB6		SAMN12568762	This study
KR4112	ΔctpA::tetAR ΔsspB::aadA		SAMN12568763	This study
	ΔCCNA_01553::hyg pAB6			·
KR4092	 ΔctpA::tetAR ΔsspB::aadA		SAMN12568761	This study
	ΔCCNA_03733::hyg pAB6			
KR4090	ΔctpA::tetAR ΔsspB::aadA		SAMN12568759	This study
	Δ <i>fur::hyg</i> pAB6			
KR4007	Δ/pxC::tetAR ΔsspB::aadA pZIK133			This study
I/D 4000	A leve Overte tA D. A en a Devente dA			This stands
KR4008	ΔlpxC::tetAR ΔsspB::aadA			This study
L/D 4000	ΔCCNA_00497::hyg pZIK133	D		- 1
KR4223	ΔlpxC::tetAR ΔCCNA_00497::hyg pZIK133	Parent strain for isolating KR4224 and		This study
I/D 4000	A leve Overte tA D. A en a Devente dA	KR4225		This stands
KR4009	ΔlpxC::tetAR ΔsspB::aadA			This study
1/5 1010	ΔCCNA_01553::hyg pZIK133			
KR4010	ΔlpxC::tetAR ΔsspB::aadA			This study
	ΔCCNA_03733::hyg pZIK133			
KR4091	ΔlpxC::tetAR ΔsspB::aadA		SAMN12568760	This study
	Δfur::hyg pZlK133			
KR4113	∆ctpA::tetAR ∆sspB::aadA		SAMN12568767	This study
	ΔCCNA_00497::hyg			
KR4114	∆ctpA::tetAR ∆sspB::aadA		SAMN12568768	This study
	ΔCCNA_01553::hyg			
KR4104	ΔctpA::tetAR ΔsspB::aadA		SAMN12568766	This study
	ΔCCNA_03733::hyg			
KR4102	ΔctpA::tetAR ΔsspB::aadA		SAMN12568764	This study
	∆fur::hyg			
KR4103	ΔlpxC::tetAR ΔsspB::aadA		SAMN12568765	This study
	Δfur::hyg			
KR4176	ΔctpA::tetAR ΔsspB::aadA			This study
	Δfur::hyg pZIK175			
KR4270	ΔctpA::tetAR ΔsspB::aadA			This study
	Δ <i>fur::hyg</i> pZIK197			
KR4177	ΔctpA::tetAR ΔsspB::aadA			This study
	Δfur::hyg pXCERN-2			
KR4178	ΔlpxC::tetAR ΔsspB::aadA			This study
	Δfur::hyg pZIK175			

KR4271	ΔlpxC::tetAR ΔsspB::aadA		This study
KR4179	Δfur::hyg pZlK197 ΔlpxC::tetAR ΔsspB::aadA		This study
KR4179	Δfur::hyg pXCERN-2		This study
KR4180	ΔctpA::tetAR ΔsspB::aadA		This study
	ΔCCNA_03733::hyg pZIK174		·
KR4181	ΔctpA::tetAR ΔsspB::aadA		This study
	ΔCCNA_03733::hyg pXCERN-2		
KR4182	ΔctpA::tetAR ΔsspB::aadA		This study
	ΔCCNA_00497::hyg pZIK172		
KR4183	ΔctpA::tetAR ΔsspB::aadA		This study
	ΔCCNA_00497::hyg pXCERN-2		
KR4148	ΔlpxC::tetAR ΔsspB::aadA	Re-introduction of	This study
	Δfur::hyg pZIK133	plasmid for	
I/D 44 40	A	complementation	- 1.
KR4149	∆lpxC::tetAR ∆sspB::aadA		This study
KD4450	Δfur::hyg pJS14	Do introduction of	This street
KR4150	ΔctpA::tetAR ΔsspB::aadA ΔCCNA 03733::hyg pAB6	Re-introduction of plasmid for	This study
		complementation	
KR4151	ΔctpA::tetAR ΔsspB::aadA	complementation	This study
101	ΔCCNA_03733::hyg pJS14		This study
KR4264	NA1000 pZIK200		This study
KR4147	NA1000 pZIK171		This study
KR4170	NA1000 pZIK179		This study
KR4489	ΔCCNA_01217		This study
KR4549	ΔCCNA_01217 vanA::01217::FLAG	pKR438 integrated	This study
KR4450	ΔCCNA_01218		This study
KK4450	\(\text{LCCNA_01218} \)		This study
KR4505	ΔCCNA_01218 vanA::01218::FLAG	pKR435 integrated	This study
KR4430	ΔCCNA_01219		This study
KR4501	ΔCCNA_01219 vanA::01219::FLAG	pKR436 integrated	This study
EK720	ΔCCNA_01220		(Stankeviciute
(KR443 1)	_		et al., 2019)
KR4530	ΔCCNA_01220 vanA::01220::FLAG	pKR437 integrated	This study
KR4517	Δfur::hyg ΔsspB::aadA		This study
	ΔCCNA_01217		

KR4551	Δfur::hyg ΔsspB::aadA ΔCCNA 01217 vanA::01217::FLAG	pKR438 integrated		This study
KR4442	Δfur::hyg ΔsspB::aadA ΔCCNA 01218			This study
KR4503		pKR435 integrated		This study
KR4438	Δfur::hyg ΔsspB::aadA ΔCCNA_01219			This study
KR4513	Δfur::hyg ΔsspB::aadA ΔCCNA_01219 vanA::01219::FLAG	pKR436 integrated		This study
KR4439	Δfur::hyg ΔsspB::aadA ΔCCNA_01220			This study
KR4532	Δfur::hyg ΔsspB::aadA ΔCCNA_01220 vanA::01220::FLAG	pKR437 integrated		This study
KR4509	ΔlpxC::tetAR ΔsspB::aadA Δfur::hyg ΔCCNA_01217 pZlK133			This study
KR4555	ΔlpxC::tetAR ΔsspB::aadA Δfur::hyg ΔCCNA_01217 vanA::01217::FLAG pZIK133	pKR438 integrated		This study
KR4451	ΔlpxC::tetAR ΔsspB::aadA Δfur::hyg ΔCCNA 01218 pZlK133			This study
KR4527	ΔlpxC::tetAR ΔsspB::aadA Δfur::hyg ΔCCNA_01218 vanA::01218::FLAG pZIK133	pKR435 integrated		This study
KR4441	ΔlpxC::tetAR ΔsspB::aadA Δfur::hyg ΔCCNA 01220 pZlK133			This study
KR4545	ΔlpxC::tetAR ΔsspB::aadA Δfur::hyg ΔCCNA_01220 vanA::01220::FLAG pZIK133	pKR437 integrated		This study
KR4205	ΔctpA::tetAR ΔsspB::aadA suppressor isolate #3	Additional genotype in Supplementary Table 1	SAMN11107060	This study
KR4206	ΔctpA::tetAR ΔsspB::aadA suppressor isolate #8	Additional genotype in Supplementary Table 1	SAMN11107061	This study
KR4207	ΔctpA::tetAR ΔsspB::aadA suppressor isolate #16	Additional genotype in Supplementary Table 1	SAMN11107062	This study
KR4208	ΔctpA::tetAR ΔsspB::aadA suppressor isolate #21	Additional genotype in Supplementary Table 1	SAMN11107063	This study
KR4209	ΔctpA::tetAR ΔsspB::aadA suppressor isolate #32	Additional genotype in Supplementary Table 1	SAMN11107064	This study
KR4210	ΔctpA::tetAR ΔsspB::aadA suppressor isolate #36	Additional genotype in Supplementary Table 1	SAMN11107065	This study
KR4211	ΔctpA::tetAR ΔsspB::aadA suppressor isolate #38	Additional genotype in Supplementary Table 1	SAMN11107066	This study
KR4212	ΔctpA::tetAR ΔsspB::aadA suppressor isolate #40	Additional genotype in Supplementary Table 1	SAMN11107067	This study
KR4213	ΔctpA::tetAR ΔsspB::aadA suppressor isolate #43	Additional genotype in Supplementary Table 1	SAMN11107068	This study

KR4214	∆ctpA::tetAR ∆sspB::aadA	Additional genotype in	SAMN11107069	This study
	suppressor isolate #44	Supplementary Table 1		
KR4215	ΔctpA::tetAR ΔsspB::aadA	Additional genotype in	SAMN11107070	This study
	suppressor isolate #47	Supplementary Table 1		
KR4216	ΔctpA::tetAR ΔsspB::aadA	Additional genotype in	SAMN11107071	This study
	suppressor isolate #52	Supplementary Table 1		
KR4217	ΔctpA::tetAR ΔsspB::aadA	Additional genotype in	SAMN11107072	This study
	suppressor isolate #53	Supplementary Table 1		
KR4218	ΔctpA::tetAR ΔsspB::aadA	Additional genotype in	SAMN11107073	This study
	suppressor isolate #54	Supplementary Table 1		
KR4219	ΔctpA::tetAR ΔsspB::aadA	Additional genotype in	SAMN11107074	This study
	suppressor isolate #57	Supplementary Table 1		
KR4220	ΔctpA::tetAR ΔsspB::aadA	Additional genotype in	SAMN11107075	This study
	suppressor isolate #111	Supplementary Table 1		
KR4221	ΔctpA::tetAR ΔsspB::aadA	Additional genotype in	SAMN11107076	This study
	suppressor isolate #112	Supplementary Table 1		
KR4224	ΔlpxC::tetAR ΔsspB::aadA	Additional genotype in	SAMN11107077	This study
	suppressor isolate #1	Supplementary Table 2		
KR4225	ΔlpxC::tetAR ΔsspB::aadA	Additional genotype in	SAMN11107078	This study
	suppressor isolate #5	Supplementary Table 2		

Table S5, related to STAR Methods: Plasmids used in this study.

Name	Description	Reference
pJS14	Broad host-range cloning vector; high copy; chlor ^R ; pBBR1MCS derivative	(J. Skerker,
	with unique EcoRI site	unpublished)
pNPTS138	kan ^R ; sacB-containing integration vector	(M.R. Alley,
		unpublished)
pXCERN-2	For integration at P _{xylX} ; encodes xylose-inducible <i>cerulean</i> that can be	(Thanbichler
	exhcanged for gene of interest; kan ^R	et al., 2007)
pMCS-2	For integration at locus specified by insert sequence; kan ^R	(Thanbichler
		et al., 2007)
pAB6	pJS14-P _{xylX} -ctpA-3xFLAG-ssrA	(Shapland et
		al., 2011)
pZIK133	pJS14-P _{xylX} -lpxC-3xFLAG-ssrA	This study
711/170	VOEDU O D. COMA COME	-
pZIK172	pXCERN-2-P _{xylX} -CCNA_00497	This study
~7U/470	AVOLDNI O D. COMA 04552	This stocks
pZIK173	pXCERN-2-P _{xylX} -CCNA_01553	This study
pZIK174	pXCERN-2-P _{xv/X} -CCNA 03733	This study
ρΣίιν 174	PAGEININ-2-1 xylx-001VA_00133	Triis study
pZIK175	pXCERN-2-P _{xylX} -CCNA_00055 (fur)	This study
pentito	product 2 1 xyix coru = cocco (rair)	Tine etady
pZIK78	pNPTS138-CCNA_00497::hyg; for replacing CCNA_00497 with	This study
•	hygromycin resistance cassette	,
pZIK82	pNPTS138-CCNA_01055::hyg; for replacing CCNA_01055 with	This study
•	hygromycin resistance cassette	Š
pZIK81	pNPTS138-CCNA_01068::hyg; for replacing CCNA_01068 with	This study
<u> </u>	hygromycin resistance cassette	
pZIK73	pNPTS138-CCNA_01553::hyg; for replacing CCNA_01553 with	This study
	hygromycin resistance cassette	
pZIK80	pNPTS138-CCNA_03733::hyg; for replacing CCNA_03733 with	This study
	hygromycin resistance cassette	
pZIK161	pNPTS138-CCNA_00055::hyg; for replacing fur with hygromycin resistance	This study
	cassette	
pZIK134	pNPTS138-CCNA_02064::tetAR; for replacing lpxC with tetracycline	This study
	resistance cassette	
pHP45Ω-hyg	For isolating <i>hyg</i> fragment; hyg ^R ; amp ^R	(Blondelet-
		Rouault et al.,
		1997)
pKOC3	Contains <i>tetAR</i> flanked by EcoRI sites; amp ^R ; tet ^R	(Skerker et al.,
		2005)
pVMCS-4	For amplification of aacC1; gent ^R	(Thanbichler
		et al., 2007)
pMCS-4	For single integration to disrupt genomic loci; gent ^R	(Thanbichler
		et al., 2007)
pVGFPC-2	Complementation vector for expressing target genes from <i>vanA</i> locus; kan ^R	(Thanbichler
		et al., 2007)

pVGFPC-4	Complementation vector for expressing target genes from vanA locus;	(Thanbichler
	gent ^R	et al., 2007)
pVCHYC-5	Complementation vector for expressing target genes from vanA locus; tet ^R	(Thanbichler
		et al., 2007)
pFLGC-1	Vector for adding FLAG tag to the C-terminus of open reading frames;	(Thanbichler
	spec ^R	et al., 2007)
pGS74	pNPTS138-based plasmid for markerless deletion of CCNA_01217	This study
pEK406	pVCHYC-5-based complementing vector, vanA::CCNA_01217-FLAG	This study
pKR438	pVGFPC-4-based complementing vector, vanA::CCNA_01217-FLAG	This study
pKR429	pNPTS138-based plasmid for markerless deletion of CCNA_01218	This study
pKR432	CCNA_01218::FLAG in pFLGC-1	This study
pKR435	pVGFPC-2-based complementation vector, vanA::CCNA_01218-FLAG	This study
pGS76	pNPTS138-based plasmid for markerless deletion of CCNA_01219	This study
pKR433	CCNA_01219::FLAG in pFLGC-1	This study
pKR436	pVGFPC-2-based complementation vector, vanA::CCNA_01219-FLAG	This study
pEK722	pNPTS138-based plasmid for markerless deletion of CCNA_01220	(Stankeviciute
P = = =		et al., 2019)
pKR434	CCNA_01220::FLAG in pFLGC-1	This study
pKR437	pVGFPC-2-based complementation vector, vanA::CCNA-01220-FLAG	This study
pKR438	pVGFPC-4-based complementation vector, vanA::CCNA-01217-FLAG	This study
		1

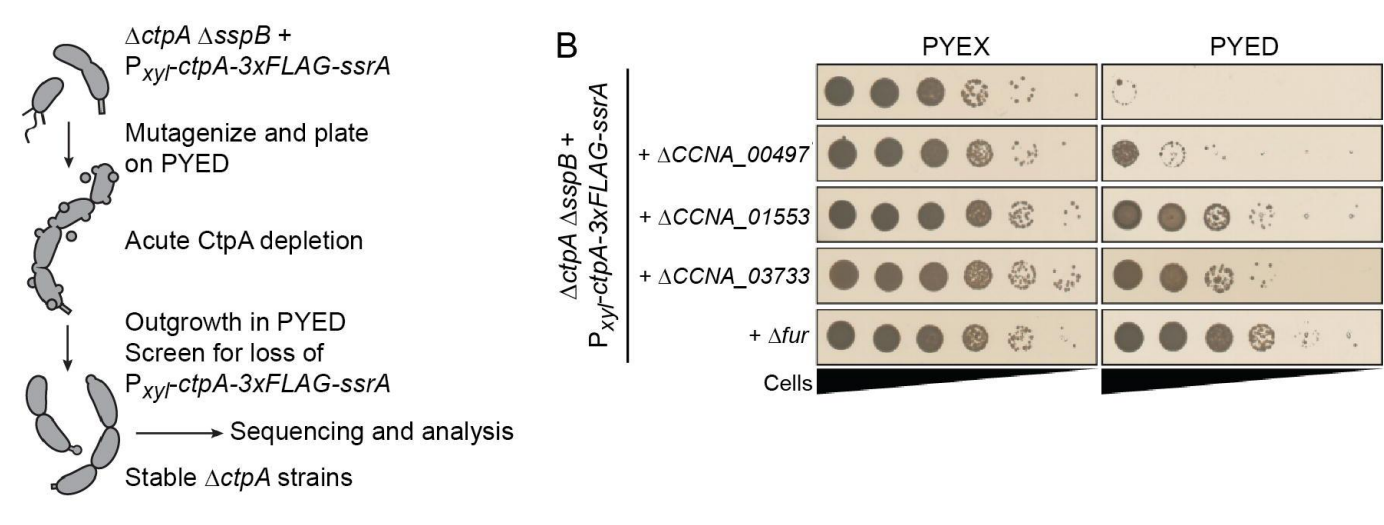
Table S6, related to STAR Methods: Primers used in this study.

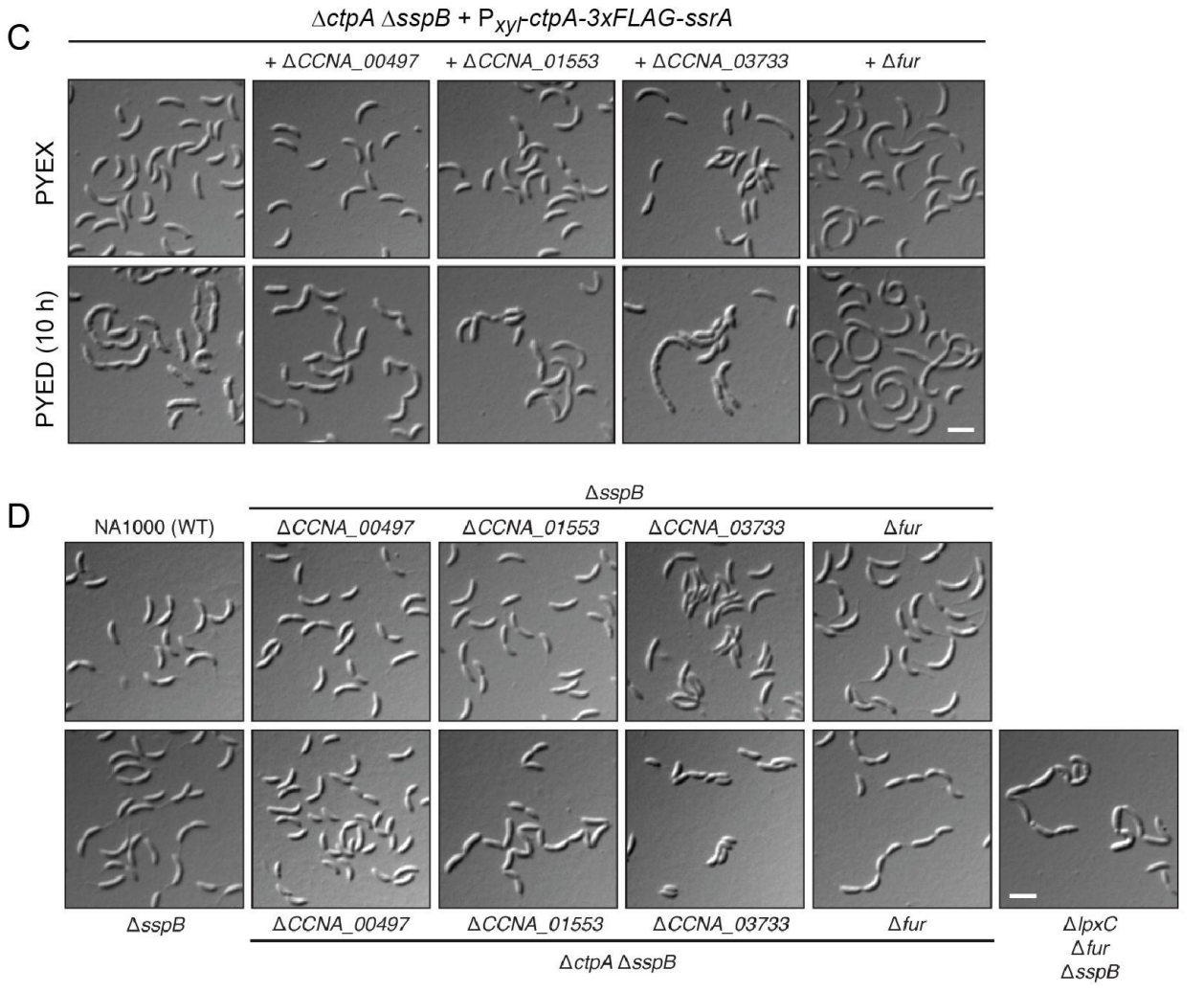
Name	Sequence (5'-3')
pJS14-PxylX	AGAACTAGTGGATCCTCACATGGTCTCGAA
PxyIX-lpxC R	ACCCGAAGCCGACACGGCGTCGTCTCCCCA
PxyIX-lpxC F	TGGGGAGACGCCGTGTCGGCTTCGGGT
lpxC-3xFLAG R	GTAGTCCATGGATCCAACCGCTTCTGCAAG
lpxC-3xFLAG F	CTTGCAGAAGCGGTTGGATCCATGGACTAC
ssrA-pJS14	CTTGATATCGAATTCTCACGCAGCGACGGC
pVCERN-2 00497 F	ACGCATATGAACAGCATTCTCCCG
pVCERN-2 00497 R	CCGGAGCTCCTAGATCGGCCGGCC
pVCERN-2 01553 F	ACGCATATGAAGCGTATGTTTGAT
pVCERN-2 01553 R	CCGGAGCTCCTAACGGGTGACGCC
pVCERN-2 03733 F	ACGCATATGGCTGCGATCTATCCG
pVCERN-2 03733 R	CCGGAGCTCTCAACGCGGCTTCGT
Pvan-fur	GAGGAAACGCATATGGATCGACTCGAAAAG
fur-pVCERN	AATTCTCCGGAGCTCTTACTCCTCCAGCGG
3xFLAG-F	cgccggcggatccatggactacaaag
3xFLAG-JS14	CTTGATATCGAATTCTCACTTGTCATCGTCATC
00497::hyg UpF	CTCACTAGTAGGACGCCCATA
00497::hyg UpR	ATCCCCGGGGCAAGGGTCGAGAC
00497::hyg DownF	ATCCCCGGGCGCCCGCTGTGG
00497::hyg DownR	AGCGAATTCACCGAGGATTTGGTT
01055::hyg UpF	CTCACTAGTGCTGGCGCTGGAAGA
01055::hyg UpR	ACCGGATCCTTGAGCGCCATGGGC
01055::hyg DownF	ACCGGATCCGATGGACGAGCGCAG
01055::hyg DownR	AGCGAATTCTACGATGACGAGTCG
01068::hyg UpF	CTCACTAGTGCGCGAGGACACCGT
01068::hyg UpR	ACCGGATCCGACGCCTGGGTGGCG
01068::hyg DownF	ACCGGATCCCAGGCGCCCATAT
01068::hyg DownR	AGCGAATTCTTGACCTGCTTGAGC
01553 UpF	AAAACTAGTATCGAGCAGGGCGTC
01553 UpR	GGCCCCGGGATCAAACATACGCTT
01553 DownF	ATCCCCGGGCCGGTGCTGACCGCA
01553 DownR	AAAGAATTCTATGCCGCCAAGCT
03733::hyg UpF	CTCACTAGTGACGCTGGCCCTTGT
03733::hyg UpR	ACCGGATCCGAAGGCGTGATCGAG

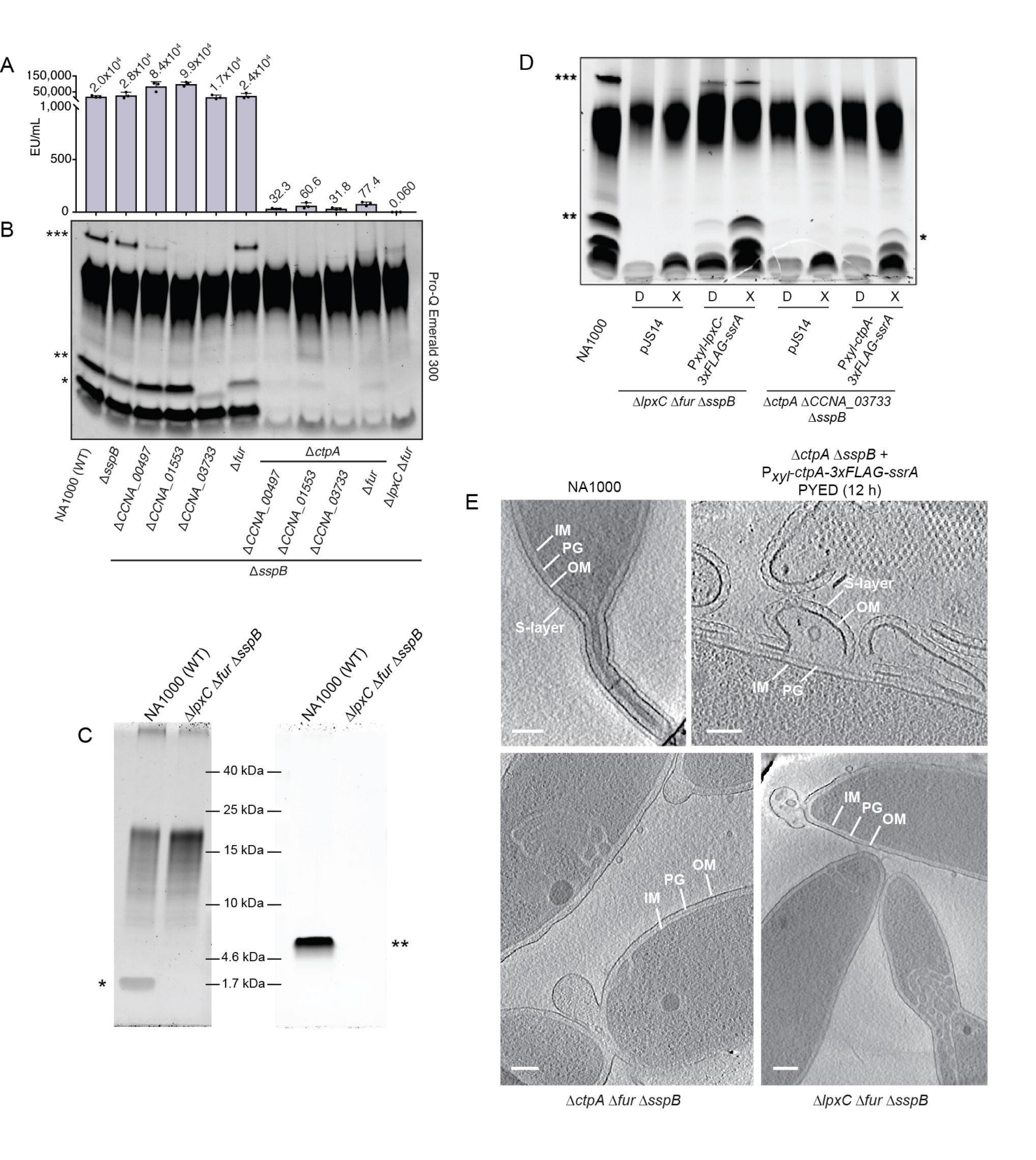
03733::hyg DownF	ACCGGATCCGCCACACAGGAT
03733::hyg DownR	AGCGAATTCATGCTCAAGGACCTC
fur UpF	CTCACTAGTAAGAGGGTGACCTCG
fur UpR	ACCGGATCCGAGCTCTACGGGATG
fur DownF	ACCGGATCCTTCGATACAGGCCTT
fur DownR	AGCGAATTCTATATGCAGGCCTTC
lpxC KO F	CTTCGAAACGGCCGATGATG
lpxC KO R	GATCAACACGCCGATGACG
lpxC UpF	CTCACTAGTTCAGATAGGCTTCGA
lpxC UpR	CATGAATTCCTCAATAACGCCGTG
lpxC DownF	CTTGAATTCCGTGTGCTGAAAATA
lpxC DownR	GACGCATGCTGGCCGCAAGCCGCG
aacC1 EcoRI F	CGCGAATTCgaattgacataagcc
aacC1 EcoRI R	GGGGAATTCgaattggccgcggcg
ctpA KO F	GAAGAAGCGCGGGATCAAGA
ctpA KO R	GTTGCCATGCTTGATGTGCA
EK897	AAGCTTGGCGCCAGCCGG
EK898	GAATTCGCTAGCTTCGGC
EK1047	gctggcgccaagcttAGGCGCTCGATCTGATCTTG
EK1048	caggaagatCGGCCTTTTTGAACTTCAC
EK1049	aagggccgATCTTCCTGGCCCTCTTC
EK1050	cgaagctagcgaattcCTTGATCGTCGGGTTCTC
EK1055	gctggcgccaagcttGGCTTCTTCCACAACTTTG
EK1056	accttgagGAGGACCCCGGACATATC
EK1057	gggtcctcCTCAAGGTCTGGAGAGAG
EK1058	cgaagctagcgaattcCGTCATCTGTCGTCCCTAC
01218 up_fwd	attgaagccggctggcgccaTGGCACGGCCATTTCGGC
01218 up_rev	tgagcccaaaGCCGTCGATCACCAGCAAG
01218 down_fwd	gatcgacggcTTTGGGCTCAAGCCGTTCG
01218 down_rev	cgtcacggccgaagctagcgGCCGTTCGACAAGCCGCG
EK1357	tactcatATGAGTAGTGAAGTTCAAAAAGGGCCG
EK1358	tactgctagcTTActtgtcatcgtcatccttgtagtcTTTCGCCAGCCAGGACTGG
EK S216	ACCCGTCTGATAAGGCTTC
EK S217	GCGAGACCGTGATCGACT
EK S238	GTAGGCAGGGTCCGACAGT
EK S239	ACCGCAAAGTTGTGGAAGAA

EK S240	ATGACCTTCCTCGACACG
EK S241	GAGTCGATCACGGTCTCG
EK S242	AGGGCTTCTTTGGCATT
EK S243	ACTTCATCGTCGGCACCTT
RecUni-1	ATGCCGTTTGTGATGGCTTCCATGTCG
RecVan-2	CAGCCTTGGCCACGGTTTCGGTACC
Nde-01218	TATATTCATATGCTTCGTCGTGCACGCCATCC
01218-Mlu	ATTATACGCGTTCCGACCAGGAACCGCAAGGC
Nde-01219	TATATTCATATGAGCCGCCTGCGCGGCCTC
01219-Mlu	TAATAACGCGTTGCCGCCGCCCCCTCTC
Nde-01220	TATATTCATATGGGGCTATTTGATAAGCACCTGGCC
01220-Mlu	AATAACGCGTGGCGCGCGCTTGAG
01217-FLAG F	CCACGATGCGAGGAAACGCATATGAGTAGTGAAGTTCAAAAAG
01217-FLAG R	AATTAAGGCGCCTGCAGGCAGCTAGCTCACTTGTCATC
01218-FLAG F	CCACGATGCGAGGAAACGCATATGCTTCGTCGTGCACG
01218-FLAG R	AATTAAGGCGCCTGCAGGCAGCTAGCTTACTTGTCATCGTC
01219-FLAG F	CCACGATGCGAGGAAACGCATATGAGCCGCCTGCGCGG
01219-FLAG R	AATTAAGGCGCCTGCAGGCAGCTAGCTTACTTGTCATCGTCATCCTTGTAG
01220-FLAG F	CCACGATGCGAGGAAACGCATATGGGGCTATTTGATAAG
01220-FLAG R	AATTAAGGCGCCTGCAGGCAGCTAGCTTACTTGTCATC

Figure 1







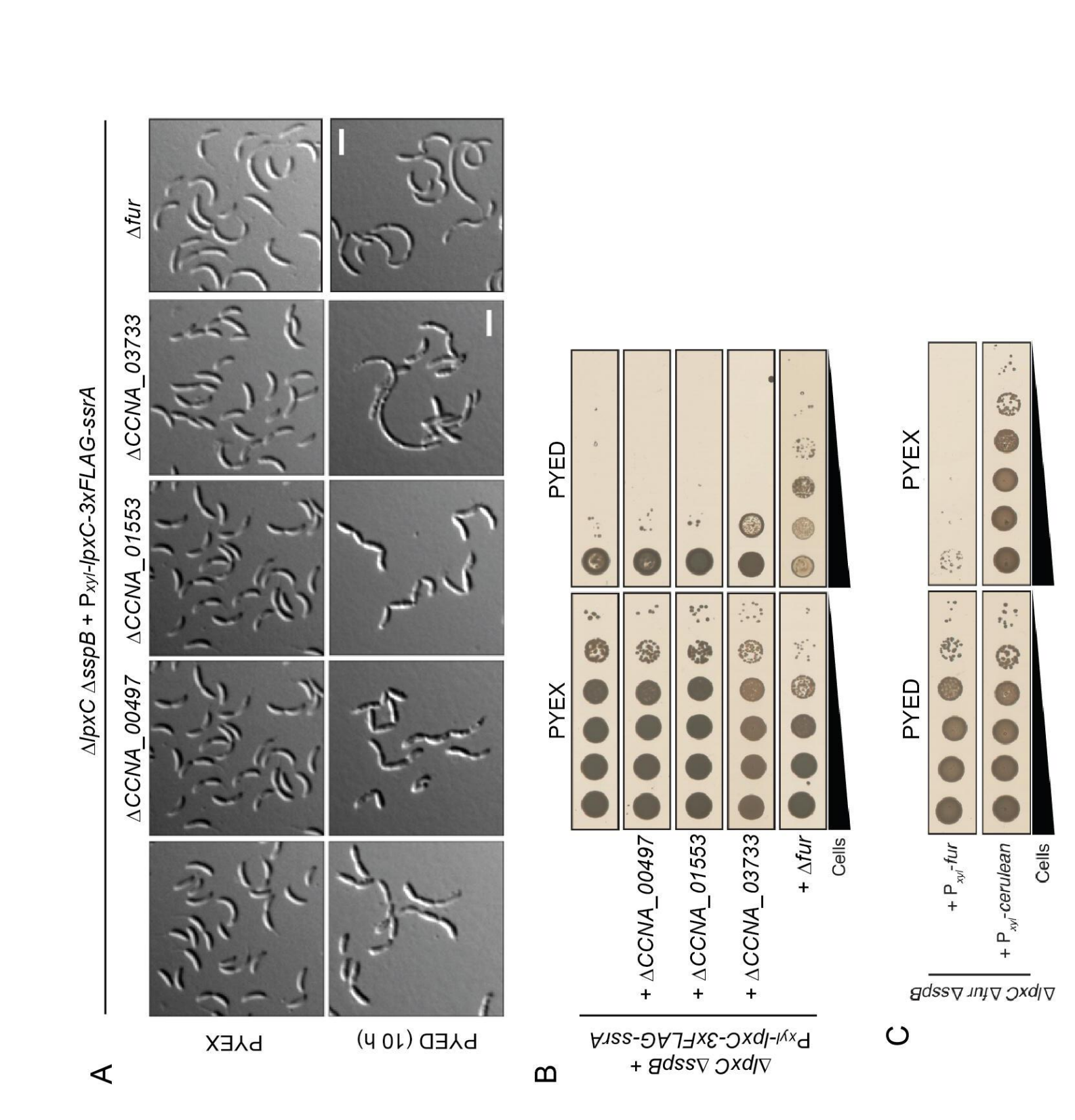
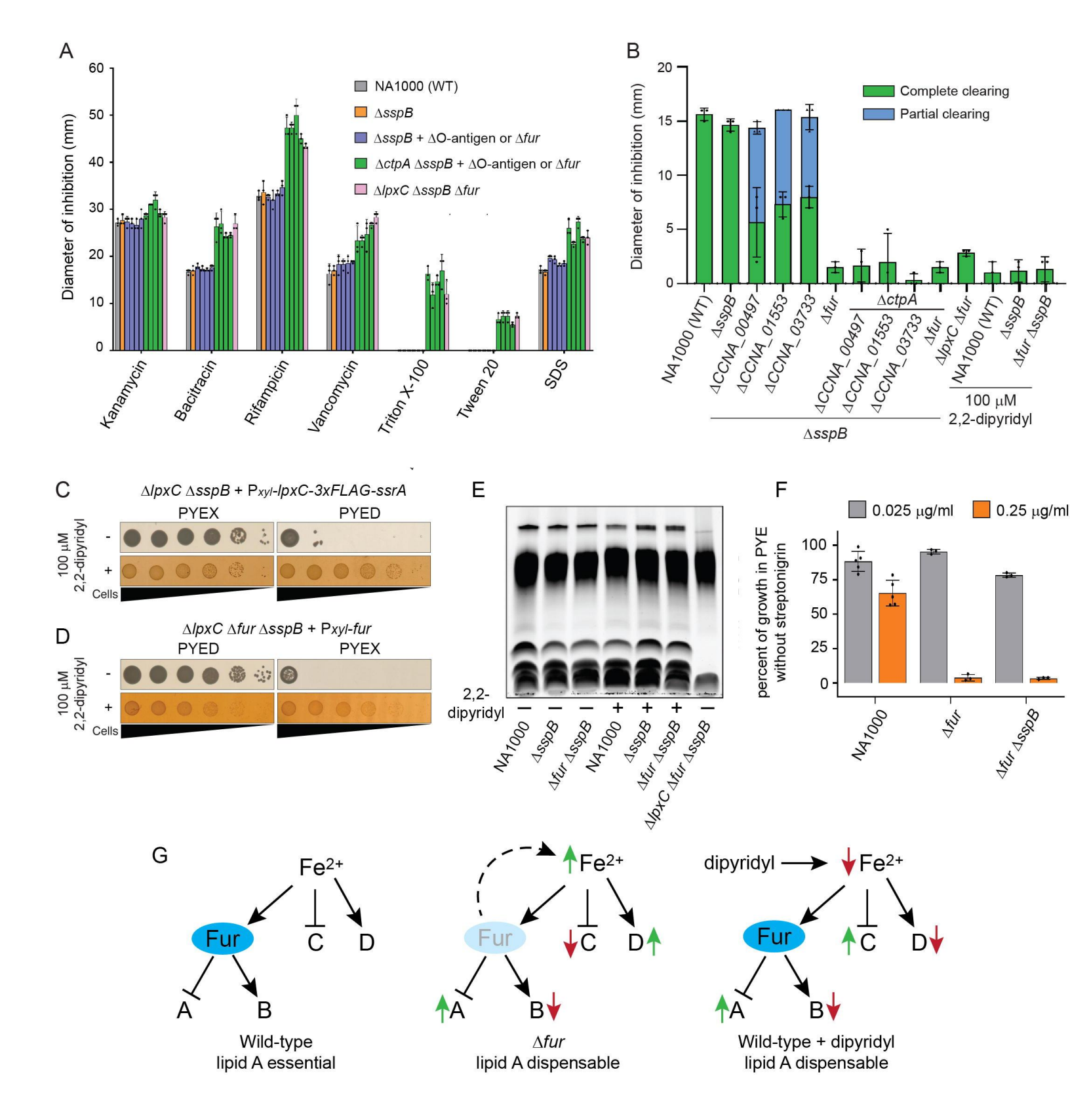
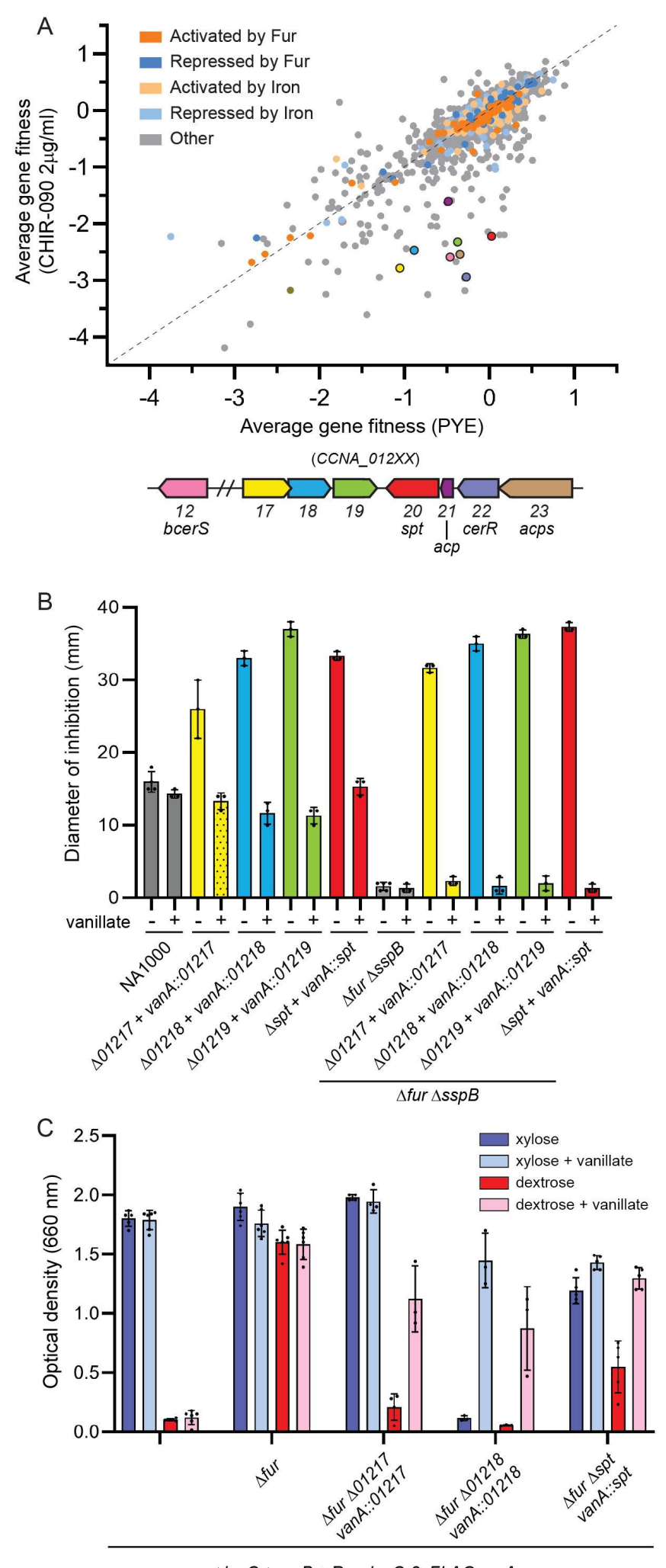


Figure 4





 $\Delta lpxC \Delta sspB + P_{xyl}-lpxC-3xFLAG-ssrA$

